Recent Approaches in Mechanistic and Kinetic Studies of Catalytic Reactions Using SSITKA Technique

Cristian Ledesma,[†] Jia Yang,[‡] De Chen,*[,†] and Anders Holmen*[,†]

[†]Department of Chemical Engineering, Norwegian University of Science and Technology (NTNU), N-7491 Trondheim, Norway
[‡]SINTEF Materials and Chemistry, N-7465 Trondheim, Norway

ABSTRACT: One of the most useful techniques to obtain valuable information on catalyzed heterogeneous reactions at, or near to, molecular level is the Steady-State Isotopic Transient Kinetic Analysis (SSITKA). Kinetic parameters of catalyst-surface reaction intermediates, such as concentration, site coverage, reactivity, and rate constants can be obtained and processed to provide valuable information about the reaction mechanism. This technique has been extensively tested in a wide range of different surface-catalyzed reactions, where the influence of different parameters on the intermediates has been studied (i.e., supports, active phases, particle size, addition of promoters). Progresses in the coupling of spectroscopic techniques and advanced modeling could greatly improve the understanding of the surface reaction mechanism and provide more reliable kinetic models. This review compiles the main goals achieved up to date in heterogeneous catalytic systems using SSITKA and analyzes the perspectives of this technique in the near future.

MS detects A and B as intermediates
IR elucidates spectator intermediates (B)

KEYWORDS: heterogeneous catalysis, reaction mechanism, isotopic transient technique, kinetics, modeling, SSITKA, infrared spectroscopy, DRIFTS
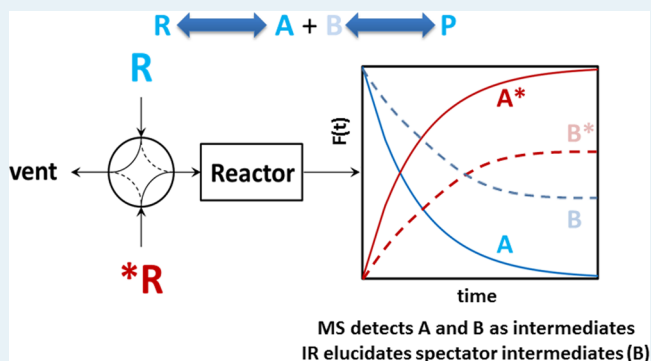
1. INTRODUCTION

Around 85−90% of the current chemical production in the industry is based on catalytic systems, and this percentage still increases steadily year after year.[1] Consequently, the understanding of the catalyst and the different pathways where it is involved become crucial. A wide range of chemical reactions and industrial processes need a heterogeneous catalyst, and a catalyst is considered a fundamental key factor to carry these processes out efficiently under practically attainable conditions. The catalytic performance can be influenced in both positive and negative ways by many physical and/or chemical processes occurring at the interface between the catalyst surface and the reactants, such as diffusion, adsorption/desorption, reaction, or surface reconstruction. Indeed, the major part of research that has been dedicated to study these phenomena, involves determining the kinetic parameters of the reactions occurring over the catalytic surface.[1−3] Particularly, most industrial processes are operated under steady-state conditions because all the parameters involved in the chemical process, such as temperature, pressure, concentration, and flow rate are time invariant. Under these conditions, the catalytic performance, the reaction order and/or the activation energy of the chemical process may be efficiently determined.[4−7] One of the most powerful techniques in steady-state conditions is the Steady-State Isotopic Transient Kinetic Analysis (SSITKA) where valuable information on catalyzed heterogeneous reactions occurring on the catalyst surface can be obtained. This technique is well-known since the late 1970s, and a wide range of publications regarding their applications are available.[4,6,8−10]

This review highlights the recent progresses in development of SSITKA in mechanistic and kinetic studies and the potential of this technique applied to an extensive range of different surface-catalyzed reactions, such as oxidation, water−gas shift (WGS), hydrogenation, or hydrogenolysis reactions, among others, to investigate the nature and the amount of surface intermediates that lead to specific products and the newest approaches and future challenges in terms of study reaction mechanisms using SSITKA combined to other techniques.

2. SSITKA METHODOLOGY

2.1. Basic Principles and General Parameters. SSITKA is a combination of steady-state and transient techniques, and as a result, the advantages from both techniques are attained. Valuable information about the catalyst surface and reaction mechanisms can be obtained at a near to molecular level under realistic, steady-state conditions, such as concentration and coverage of surface intermediates, surface residence time, intrinsic turnover frequency (TOF), surface heterogeneity, catalyst dispersion, and/or reactivity distribution.

SSITKA was broadly developed by Happel, Bennett, and Biloen.[4,6,8] Most of the work published prior to 1995 was included in a review paper on this topic by Shannon and Goodwin.[4] A common setup to carry out SSITKA experiments is depicted in Figure 1a. Typically, when the catalyst operates
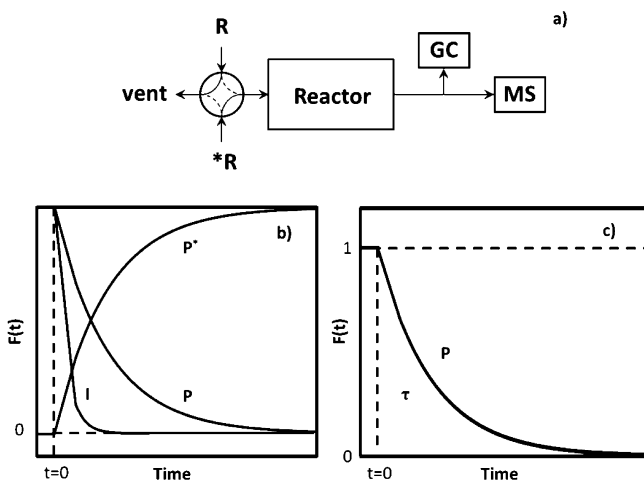

Figure 1. (a) Flow scheme of a typical SSITKA setup; (b) normalized transient curve for decaying response of the unlabeled product (P) including the inert response (I) and the increasing response of the labeled product (P*); (c) normalized transient response for decaying response indicating the graphic meaning of surface residence time (τ).

under steady-state conditions, an isotopic transient is introduced by suddenly replacing one compound with its isotope (e.g., $H_2/^{12}CO/Ar \rightarrow H_2/^{13}CO/Kr$) causing minimum effects to the system. There is also a replacement of the inert gas in order to determine the gas hold-up in the reactor. Because the reactor operates under isothermal and isobaric conditions, the catalytic surface does not suffer any change during the isotopic switch, and mechanistic studies can be carried out efficiently at these conditions using this technique. The reaction feed and the obtained products are typically analyzed and quantified by online gas chromatography (GC). The transient responses are recorded and monitored by a mass spectrometer (MS), operated under minimal fragmentation of the detected reaction species to avoid overlapping of heavier products. Figure 1b shows a typical normalized transient curve for the decaying (P) and increasing (P*) responses of the products obtained after reaction of the labeled and unlabeled reactants (R, R* respectively).

For a given reversible heterogeneous catalytic reaction at steady-state, a reactant (R) is transformed into a product (P) through an adsorbed intermediate (X). At these conditions the amounts of R, P, and X are constant.

$$R \rightleftarrows X \rightleftarrows P$$
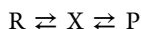
The nature of the intermediates (X) may be diverse and can be located in different subsystems, or pools, which are homogeneous or well-mixed. Irrespective of the underlying kinetic model, SSITKA permits absolute measurement and quantification of the most reactive intermediates converted into products:

$$N_p = \int_0^\infty r_p(t)\,dt \tag{2.1}$$

where N_p is the amount of adsorbed intermediates and $r_p(t)$ the reaction rate of unlabeled products.

$$r_p(t) = r_p - r_{p*}(t) \tag{2.2}$$

where r_p and $r_{p*}(t)$ are the steady-state reaction rates of the unlabeled and labeled products, respectively. The amount of adsorbed intermediates (N_p) and the mean surface residence time (τ_p) are the most general parameters obtainable from SSITKA. The average surface residence time can be obtained from the normalized transient responses as shown in Figure 1c. $F_p(t)$ and $F_{p*}(t)$ are the normalized transient responses of the unlabeled and labeled products respectively, defined as

$$F_p(t) = \frac{r_p(t)}{r_p}; \text{ where } F_p(t) = 1 - F_{p*}(t) \tag{2.3, 2.4}$$

The overall residence time of the product is obtained by the integration of the normalized transient response. Rearranging the previous equations, the calculation of the residence time yields to

$$\tau_p = \int_0^\infty F_p(t)\,dt = \int_0^\infty \frac{r_p(t)}{r_p}\,dt = \frac{N_p}{r_p} \tag{2.5}$$

2.2. SSITKA Modeling. The amount and surface lifetime of adsorbed intermediates (N_p and τ_p respectively) are the most general parameters that can be directly obtained by SSITKA experiments.[9] Additional kinetic parameters may, however, be calculated but are dependent on assumptions and specific models regarding the reactor configuration.

The reactor configurations used in SSITKA analysis can be the continuous-stirred tank reactor (CSTR) or plug-flow reactor (PFR). A CSTR configuration considers that there are no changes in composition between inside the reactor and the outlet. In addition, the composition is a function of the residence time and the reaction rate. This configuration assumes steady-state and isothermal conditions, single and irreversible first-order reactions. CSTR is commonly used to clear up the calculations and can be also applied to describe reactors operating at low conversion level. A widespread discussion in the calculations and assumptions of a CSTR model to obtain these specific parameters can be found in the review of Shannon and Goodwin.[4] The results are summarized in Table 1.

In the first model, an irreversible adsorption and first-order reaction of the reactants is considered, and the intermediates are converted into products in a single type of catalytic site. For this model, the intermediate accumulation rate can be calculated as the subtraction between the reactant inlet rate and the product outlet rate, as predicted by the mass balance. Furthermore, once the overall mean surface residence time is calculated from the expression shown in Table 1, the rate constant can be calculated. For a pseudo-first-order reaction, the turnover frequency of the reaction intermediate i (TOF_i) can be calculated as a product of the rate constant and the coverage of reaction intermediates.[10] The coverage is linked by the amount of reaction intermediates (N_i) and the overall active sites available (N_s), a parameter that can be obtained by chemisorption experiments.

In model 2, an irreversible reaction proceeding by a single pool system is shown. Thus, the same expression of the overall transient response is used. In this case, because a reversible adsorption is considered, the equation to calculate the steady-state reaction rate includes a term corresponding to the adsorption rate (r_R^a). The calculation of the surface lifetime of

Table 1. Mechanistic Models, Transient Responses, and Kinetic Parameters Obtained by SSITKA (Reproduced from Ref 4. Copyright 1995, American Chemical Society)

	reaction	adsorption	pool system	model	transient responses and kinetic parameters
1	irreversible	irreversible	single	$R \xrightarrow{r_R} X \xrightarrow[F_P(t)]{r_P} P$	$F_P(t) = e^{-t/\tau_X}$; $r_R = r_P$ $\tau_X = \dfrac{N_X}{r_P}\tau_P$; $k = \tau_i^{-1}$ $TOF_i = \dfrac{r_i}{N_S} = \tau_i^{-1} \cdot \dfrac{N_i}{N_S} = k \cdot \theta_i$
2	irreversible	reversible	single	$R \underset{r_R^d}{\overset{r_R^a}{\rightleftarrows}} X \rightarrow P$	$F_P(t) = e^{-t/\tau P}$; $r_P = r_R - r_R^a$ $\tau_X = \dfrac{N_X}{r_P + r_R^d} = \tau_P$
3	irreversible	irreversible	multiple in series	$R \rightarrow X_i \rightarrow P$	$F_P(t) = \displaystyle\sum_{i=1}^{n} \dfrac{\tau_i^{n-1}}{\Pi_{j=1,j\neq i}^{n}(\tau_i - \tau_j)} e^{-t/\tau_i}$ $\tau_P = \displaystyle\sum_{i=1}^{n} \tau_i$
4	irreversible	reversible	multiple in series	$R \underset{r_R^d}{\overset{r_R^a}{\rightleftarrows}} X_1 \rightarrow X_i \rightarrow P$	$F_P(t) = \displaystyle\sum_{i=1}^{n} \dfrac{\tau_i^{n-1}}{\Pi_{j=1,j\neq i}^{n}(\tau_i - \tau_j)} e^{-t/\tau_i}$ $\tau_1 = \dfrac{N_1}{r_P + r_R^d}$; $\tau_{i,i>1} = \dfrac{N_i}{r_P}$ $\tau_P = \displaystyle\sum_{i=1}^{n} \tau_i$
5	irreversible	irreversible	multiple in parallel	$R \rightarrow X_i \rightarrow P$ $R \rightarrow \vdots \rightarrow P$ $R \rightarrow X_n \rightarrow P$	$F_P(t) = \displaystyle\sum_{i=1}^{n} x_i e^{-t/\tau_i}$ $x_i = \dfrac{N_i}{\sum_{i=1}^{n} N_j}$; $\tau_P = \displaystyle\sum_{i=1}^{n} x_i \tau_i$
6	irreversible	reversible	multiple in parallel	$R \underset{r_{R,i}^d}{\overset{r_{R,i}^a}{\rightleftarrows}} X_i \xrightarrow{r_{i,p}} P$ $R \rightleftarrows \vdots \rightarrow P$ $R \rightleftarrows X_n \rightarrow P$	$F_P(t) = \displaystyle\sum_{i=1}^{n} x_i e^{-t/\tau_i}$ $x_i = \dfrac{N_1}{\sum_{i=1}^{n} N_j}$; $\tau_i = \dfrac{N_i}{r_{i,p} + r_{R,i}^d}$ $\tau_P = \displaystyle\sum_{i=1}^{n} x_i \tau_i$

the intermediates includes a term referred to the rate of desorption.

Models 3 and 4 consider irreversible reaction and irreversible or reversible adsorption of the reactants, respectively. In these cases, the reaction proceeds through multiple pools in series, where the output of the first intermediate pool will be the feed to the next intermediate pool. The overall surface residence time from the general case is determined by the summation of the residence time on each pool. Extending the mass balance, the exponential equation of the normalized transient response includes an additional term which includes the surface residence time in each pool, as shown in Table 1.

Models 5 and 6 are typically the case for a nonhomogeneous catalyst surface, with multiple sites with varying activity, or multiple pathways to the same product, as shown in Table 1. Considering all of these pathways as irreversible first order reactions, the overall transient response is given by the summation of an exponential function which is multiplied by the fractional number (x_i) of the intermediates (N_i) in the ith pool at steady-state conditions. The overall surface lifetime of the intermediates is obtained as the summation of the residence time of each pool multiplied by the fractional number of the

intermediates over the surface. As seen in models 2 and 4, if readsorption occurs, the adsorption/desorption rate constants must be included in the calculation of the parameters.

The differences between the kinetic models can easily be distinguished in a plot of $F_p(t)$. The two pool models are shown along with the one-pool irreversible first-order reaction, as depicted in Figure 2.[4] The series pool model does not decrease
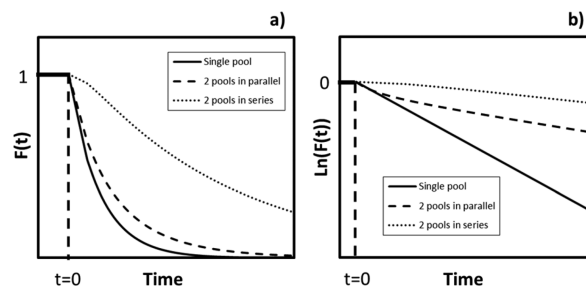

Figure 2. Comparison of the transient response (a) and logarithmic transient response (b) of single pool, two pools in series and two pools in parallel models.

immediately after the switch, as is the case for the two other models. The differences between the other two are best seen in a logarithmic plot (Figure 2b), where the single pool model gives a straight line, whereas the parallel pool model deflects. For the single pool model, the slope in the logarithmic plot is equal to $-1/\tau_P$. A wide discussion and comparative within these models can be found elsewhere.[4]

These models can be applied to characterize those processes that include a set of unidirectional steps. These include such reactions as the cracking of petroleum compounds and their oxidation.[11−13] The presence of elementary reversible reactions, such as in the synthesis of ammonia,[14−17] dehydrogenation,[18−21] or isomerization reactions,[22−25] cannot be described by the equations listed in Table 1.

The different reaction systems presented in Table 1 have excluded reversible elementary steps because of the impossibility to obtain analytical solutions for the product transient response. However, numerical methods based on nonlinear least-squares regression have been developed to obtain the kinetic parameters on the basis of reaction systems including reversible steps.[26] The combination of these numerical methods with the catalyst performance and the transient responses are used to obtain estimations of the kinetic parameters through nonlinear multiresponse regression analysis. The development of studies based on transient isotopic tracing has facilitated the determination of fundamental kinetic parameters in heterogeneous catalysis, including reversible reaction paths.[26] Mainly, these studies have been focused on the establishment of mechanisms involved and the construction of kinetic rate equations with more than an empirical basis. Moreover, the study allows assessing the magnitudes of individual step velocities and concentrations of adsorbed surface species regardless of the overall kinetics.[26]

2.3. Limitations and Corrective Techniques.

2.3.1. Chromatographic Effect. The adsorption of reactants must be taken also into account. The components can adsorb not only on the catalyst surface but also throughout the whole reactor system. This will lead to a delay in the change of isotope composition in the gas phase. The chromatographic effects should be kept small in order to avoid interference with the intrinsic kinetics. Increasing the space velocity of the reactants decreases the chromatographic effect. It has been pointed out that the chromatographic effect can be neglected if the area between the response of the reactant and inert is less than 20% of the area between the response of the product and inert. Additionally, it has been suggested that the chromatographic effect could be corrected using the equation:[27−29]

$$\tau_{P,corrected} = \tau_{P,measured} - x \cdot \tau_{P,reactant} \qquad (2.6)$$

The value of x in eq 2.6 varies among the different users[27−29] but is typically 0.5, which was proposed by Biloen and co-workers.[8]

2.3.2. Readsorption and Gas Phase Hold-Up. The product response curves in SSITKA experiments are delayed due to readsorption and hold-up in the gas phase.[4,30] The overall surface lifetime measured experimentally includes the true residence time for intermediates leading to products and the residence times due to the gas phase (hold-up) and due to readsorption. There are different existing methods to calculate the real surface residence time for the reaction. The most common procedure to correct the hold-up is the addition of an inert gas to the unlabeled or labeled reactant, as mentioned previously. The area under the inert gas transient is a direct

measure of its residence time, because the inert gas is not adsorbed on the surface. Values for the hold-up on the surface due to interparticle readsorption cannot be obtained directly, but it is possible to minimized these values by decreasing the length of the catalyst bed or the contact time between the reactants and the catalyst. An increase in the surface reaction residence time (τ_P) with increasing bed length is a strong evidence of the presence of reversible.[30] The easiest method to assess the real surface residence time when readsorption occurs is to carry out the reaction under different contact times and extrapolate to a value of zero residence time, as shown in Figures 3a and 3b. Ali and co-workers determined the true
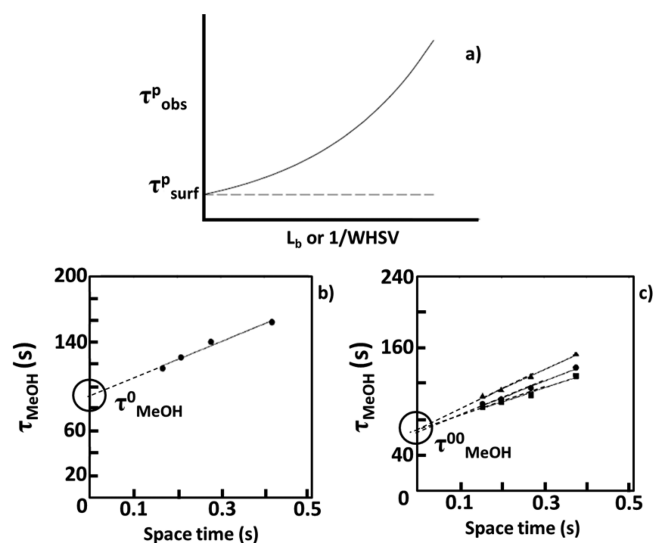

Figure 3. (a) Experimental calculation of the mean surface-residence time in the presence of interparticle readsorption; (b) τ_{MeOH} vs space time during steady-state MeOH synthesis at 493 K; (c) τ_{MeOH} vs space time at constant average P_{MeOH} (▲= 26.5 Pa, ● = 38.5 Pa, ■ = 50.5 Pa) during steady-state MeOH synthesis at 493 K on Pd. (Reproduced from ref 30. Copyright 2006, World Scientific Publishing Co.)

surface residence time considering both inter- and intraparticle readsorption for methanol synthesis on Pd/SiO₂.[31] As shown in Figure 3c, the surface residence time of intermediates producing methanol (τ_{MeOH}) was adjusted holding methanol partial pressure constant. The parameter τ^{00}_{MeOH} represents the extrapolation of the residence time to zero space time at different MeOH partial pressures.[31]

2.3.3. Isotopic Exchange H₂/D₂. In order to obtain accurate values of the kinetic parameters, the maintenance of the steady-state conditions is critical. Hence, isotope effects on reaction conditions are not allowed. The thermodynamic and kinetic distinctions due to the relatively large mass differences and the bonding energies between hydrogen isotopes are significantly high and the steady-state conditions can no longer be maintained. As a consequence, the kinetic rates and surface concentrations are substantially changed after the hydrogen/deuterium isotopic exchange.[32] Nevertheless, isotopic H₂−D₂ exchange can provide information about the characterization of the active surface when hydrogen chemisorption is not possible due to hydrogen spillover. Basallote and co-workers[32] described the use of H₂−D₂ SSITKA switches in the characterization of the active surface of Pt/CeO₂ catalyst to evaluate the number of active sites taking part in the exchange process, especially in the gas phase, and with supports. Deuterium isotopic pulse tracing

into a steady-state $CO/H_2/C_2H_4$ flow has been also useful in combination with in situ spectroscopic techniques to study the hydroformylation and hydrogenation of ethylene over a Mn–Rh/SiO₂ catalyst at 513 K and 0.1 MPa.[33] The steady-state rate of hydrogen desorption coupled with compartment models allowed the calculation of the complete assortment of kinetic parameters. Hydrogen desorption was estimated by the HD transient assuming that the H and D coverages are similar when the production rates of HD, D_2, and H_2 are the same.

2.3.4. Isotopic Exchange $^{16}O_2/^{18}O_2$. The possible transfer between oxygen atoms present in the gas phase, the surface of the catalyst, and/or the catalyst bulk makes the determination of surface kinetic parameters using oxygen isotopic exchange a challenging measurement. Nevertheless, Peil and co-workers demonstrated that it is possible to quantify the lattice oxygen diffusivity and total oxygen uptake by SSITKA.[34] Other examples of the use of SSITKA with oxygen isotopic exchange can be found in the literature, such as the oxidation of acrolein[35−40] or oxidative dehydrogenation of hydrocarbons[18−21] where SSITKA was applied to determine the nature of the active intermediates and the oxygen reaction mechanism. In order to get more information about the kinetic parameters, isotopic replacement of oxygen may be combined with other isotopic exchanges, such as $^{12}C/^{13}C$.[34,41,42]

2.4. Advanced Mathematical Analysis. 2.4.1. Deconvolution Methods. The catalytic surface can be characterized by the measurement of the intrinsic reactivity of its active sites. This reactivity can be obtained by the calculation of the reactivity distribution function $(f(k))$ from the isotopic transient curve, but it is only valid for pseudo-first-order reactions where no readsorption occurs. The reactivity distribution is dependent on the parameter k, which is a measure of site activity. In order to calculate $f(k)$, a numerical deconvolution method must be used, such as the parametric or the nonparametric method. The parametric method includes a model to calculate $f(k)$, but an assumption of its functional form is needed.[43] For this reason, nonparametric methods are preferred because no assumption of a specific form of the function is required. Currently, some of the studies carried out by SSITKA have included the calculation of the reactivity distribution using two different types of nonparametric methods: the inverse-Laplace-transform technique (ILT) and the Tikhonov−Fredholm method (T−F).

The ILT method defines the formation rate of a product P, named $r*_p(t)$, as the Laplace transform of $N_p \cdot k \cdot f(k)$. The isotopic transient function of the product formation rate is expressed as follows for a pseudo-first order reaction:

$$r_p^*(t) = N_P \int_0^\infty k e^{-kt} f(k) \, dk \qquad (2.7)$$

where N_p is the surface concentration of the intermediates leading the product P. $f(k)$ can be obtained by using the inverse-Laplace transform to $r*_p(t)$. Despite, the value of $f(k)$ is more commonly obtained from the T−F method, since it can be extracted more accurately from $r*_p(t)$ by using the Tikhonov regularization of eq 2.7.[43] Moreover, this method can retrieve substantially the reactivity distribution despite the presence of small amounts of noise. It must be pointed out that, as mentioned before, these methods are not able to take into account possible readsorption processes in the reaction mechanism. Figure 4 shows an example of CO_2 transient in the CO selective oxidation over Pt/γ-Al₂O₃ (Figure 4a) and the reactivity distribution function obtained from the T−F method
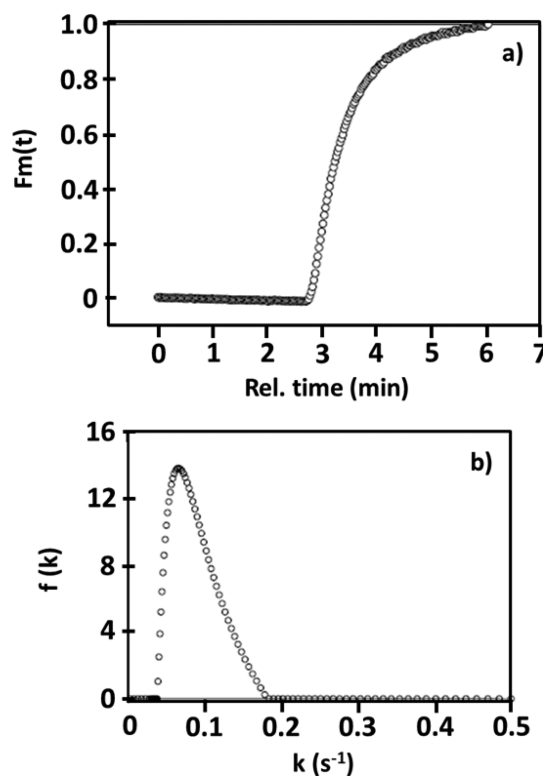

Figure 4. (a) Normalized isotopic transient of $^{13}CO_2$ and (b) reactivity distribution obtained by T−F for the selective CO oxidation on Pt/γ-Al₂O₃. (Reproduced from ref 30. Copyright 2006, World Scientific Publishing Co.)

as a function of site activity (k) for the CO_2 transient (Figure 4b).[30]

2.4.2. Convolution Methods. Linear convolution systems may use advanced analysis methods in SSITKA studies. These methods include parametric and nonparametric kinetic analysis to determine some kinetic parameters of pseudo-first-order reactions.[44] The relationship between the step input responses in a PFR model is given by the following linear convolution integral, considering a differential bed length:

$$F_m^{*P}(t) = \int_0^t [D_t\{F_c^{*P}(t-\zeta)\} \cdot F_m^{+I}(\zeta)] \, d\zeta \qquad (2.8)$$

where ζ is a convolution time variable; $D_t\{F*Pc(t-\zeta)\}$ is the convolution form of the first derivative $(D_t = d/dt)$ of the catalyst transient response $(Fc*P(t))$; F^{+I}_m is the measured intermediate (I) transient response and $F^{+I}_m(\zeta)$ is the convolution form of $F^{+I}_m(t)$. The linear convolution relationship for the transient response is presented by eq 2.9:

$$F_m^{*P}(t) = 1 + \int_0^t [D_t\{F_c^P(t-\zeta)\} \cdot (1 - F_m^{-I}(\zeta))] \, d\zeta \qquad (2.9)$$

The combination of eqs 2.8 and 2.9 suggests a method to validate a model of reaction pathway and the kinetics involved.[44] These equations allow the creation of the transient response that characterizes the surface behavior and the inert tracer transient response that describes the gas-phase behavior of the reactor system. Despite, the establishment of an analytical relationship within the equations is not possible, and as a consequence, the determination of the calculated transient response from the measured one must be assumed

and tested using a model. In addition, as also occurred with deconvolution methods, convolution methods can only describe pseudo-first-order processes, and readsorption cannot be considered.

2.4.3. PFR Reactor Modeling. If the reaction mechanism contains reversible reaction steps of reactants or products, such as readsorption processes, the CSTR approach is no longer valid, and a PFR model should be applied. The PFR reactor model is represented by differential equations for the components that participate in the isotopic substitution.[44] Although the continuity equations for the CSTR approximation are ordinary differential equations in time, the PFR approximation introduces an additional spatial-position variable, resulting in a set of partial differential equations in time and space. Analytical solutions can hardly be obtained, and the set of equations has to be solved numerically using differential or integral conditions, depending on the variation of the reaction rates throughout the catalyst bed. The major benefits of PFR modeling compared to deconvolution and convolution methods are that it can describe more complex processes than pseudo-first-order reactions, and this model may take into account internal diffusion limitations, especially in microporous catalysts with fast heterogeneous reaction. A detailed description of the transient curve using PFR modeling applied to Fischer–Tropsch synthesis is discussed below.[27,45−47]

The general equation for labeled gaseous component X' is represented by eq 2.10 and for the labeled surface component Y' by eq 2.11:

$$\frac{\partial C_{X'}}{\partial t} + \frac{1}{\tau}\frac{\partial C_{X'}}{\partial x} = \frac{\rho_b}{\varepsilon_b}R_{w,X'} \tag{2.10}$$

$$\frac{\partial L_{Y'}}{\partial t} = R_{w,Y'} \tag{2.11}$$

The initial condition for labeled compound based on isotopic switch from unlabeled reactant to labeled reactant:

Initial conditions: $t = 0$ $C_{X'} = C_{Y'} = 0$;

Boundary conditions: $t > 0$, $x = 0$, $C_{reactant'}$ = input function (t);

                   $t > 0$, $x = 0$, $C_{product'} = 0$;

where $C_{X'}$ is gas phase concentration mol/m³ gas; $L_{Y'}$ is surface concentration mol/kg$_{cat}$; τ is the residence time in s; t is time in s; ε_b is the porosity of the bed m³ gas/m³ bed; ρ_b is the density of the catalysts bed in kg/m³ bed; $R_{w'}$ is the reaction rate of different species in mol/kg$_{cat}$; x is the axial position in the catalyst bed (dimensionless). The residence time (τ) is calculated as $\tau = (\varepsilon_b)/(F_V)V_R$, where V_R is the volume of the catalyst bed in m³, F_V is the total volumetric flow rate in m³/s at reaction conditions. The input function is the transient response of the inert tracer Ar.

As an example of transient curve modeling for CO hydrogenation, modeling of CO transient curve provides information on the kinetics of CO adsorption, namely, CO adsorption, desorption rate constant and the conversion of surface adsorbed CO. Modeling of CH₄ transient curve helps to differentiate possible reaction routes for methane formation and provide kinetic rate parameters involved. The CO and CH₄ transient curves were modeled simultaneously using a PFR model as was described by Van Dijk on cobalt catalysts.[27] Scheme 1 shows one possible reaction pathway.

The continuity equations for mechanism shown in Scheme 1 are shown as follows:

Scheme 1. Possible Reaction Pathway for Methane Formation (Reproduced from Ref 47. Copyright 2013, Elsevier.)
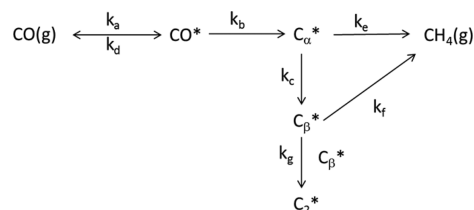
$$\frac{\partial C_{13CO}}{\partial t} + \frac{1}{\tau}\frac{\partial C_{13CO}}{\partial x} = -k_a C_{13CO} + \frac{\rho_b}{\varepsilon_b}k_d L_{13CO} \tag{2.12}$$

$$\frac{\partial L_{13CO}}{\partial t} = \frac{\varepsilon_b}{\rho_b}k_a C_{13CO} - k_d L_{13CO} - k_b L_{13CO} \tag{2.13}$$

$$\frac{\partial C_{13CH_4}}{\partial t} + \frac{1}{\tau}\frac{\partial C_{13CH_4}}{\partial x} = \frac{\rho_b}{\varepsilon_b}(k_e L_{13C_\alpha} + k_f L_{13C_\beta}) \tag{2.14}$$

$$\frac{\partial L_{13C_\alpha}}{\partial t} = k_b L_{13CO} - k_c L_{13C_\alpha} - k_e L_{13C_\alpha} \tag{2.15}$$

$$\frac{\partial L_{13C_\beta}}{\partial t} = k_c L_{13C_\alpha} - k_f L_{13C_\beta} - k_g L_{13C_\beta} L_{13C_\beta} \tag{2.16}$$

where C_{13CO} and C_{13CH4} are gas phase concentrations for ^{13}CO and $^{13}CH_4$; L_{13CO}^{SS}, $L_{13C\alpha}^{SS}$ $L_{13C\beta}^{SS}$ are surface concentrations of adsorbed CO*, C_α* and C_β*, respectively; k_a, k_d, k_b, k_c, k_e, k_f, k_g are rate constants involved in CO adsorption, activation and CH₄ production pathway. ρ_b and ε_b are characteristic parameters for the catalyst bed; τ depends on the total gas flow rate and catalyst bed.

Known parameters:

- ρ_b, ε_b, and τ are known for certain packed catalyst bed at given reaction conditions
- Steady-state gas phase CO and CH₄ concentration (L_{13CO}^{SS}, L_{13CH4}^{SS})
- Total surface C₁ concentration ($L_{13C\alpha}^{SS} + L_{13C\beta}^{SS}$) measured by SSITKA
- The rate constants k_a, k_d, k_b, k_c, k_e, k_f, k_g are interrelated based on the steady-state assumption. $(\partial L_{13CO}^{SS})/(\partial t) = 0$, $(\partial L_{13C\alpha}^{SS})(\partial t) = 0$, $(\partial L_{13C\beta}^{SS})(\partial t) = 0$ and $k_b L_{13CO} = R_{13CO}^{SS}$. With four equations, the independent rate constants are minimized to two, here we chose k_a and k_e as input.

Therefore, the input parameters are minimized to three parameters: k_a, k_e and $L_{13C\alpha}^{SS}$.

The output of the model contains the amount of two carbon pools: $L_{13C\alpha}^{SS}$, $L_{13C\beta}^{SS}$, and rate constants involved in the CO adsorption (k_a, k_d), activation (k_b), methane formation (k_c, k_e, k_f) and C−C bond formation (k_g). Figure 5 shows a typical simulated transient curve for ^{13}CO and $^{13}CH_4$.

The transient modeling can not only be applied to C₁ reaction but also to more complicated reaction system. For instance, it can be used to study kinetics of the production of C$_{2+}$ hydrocarbons in CO hydrogenation. The prerequisite is that possible reaction pathways have to be proposed first[48] (Figure 6). Transient kinetic modeling allows us to first distinguish different reaction routes. Once the reaction route is determined, it can be used to determine kinetic parameters, such as olefin readsorption and termination rate constant,
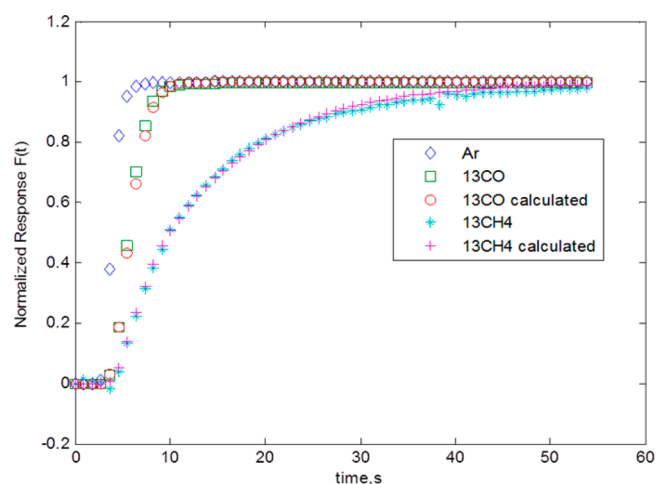
Figure 5. Example of simulated transient curve for ^{13}CO and $^{13}CH_4$.
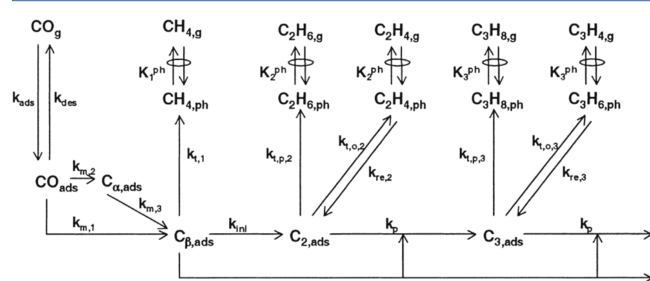

Figure 6. Reaction pathway for methane and higher hydrocarbons formation. (Reproduced from ref 48. Copyright 2001, Elsevier.)

paraffin termination rate constant. Therefore, the olefin readsorption and chain growth and termination reactions can be studied kinetically, which is very important for tuning product selectivity.

2.5. Applications. SSITKA has provided much information about the understanding of the reaction pathway of many surface-catalyzed reactions. The review of Shannon and Goodwin compiles the chemical reactions studied by SSITKA prior to 1995.[4] Table 2 includes a compilation of the most important catalyzed reactions and processes studied by SSITKA up to date. The reported processes include mainly the study of mechanisms, the presence and implications of site heterogeneity, the role of chemical promoters and the effect of operational conditions on surface coverage of intermediates among others. Table 2 does not include the works regarding the application of SSITKA in the Fischer−Tropsch synthesis or its combination to other methods because those studies will be discussed extensively in section 3.

The determination of different kinetic parameters, such as surface coverage of the main intermediates or their turnover frequency by SSITKA plays a turning role in the determination of reaction pathways. These parameters were crucial to elucidate the reaction mechanism of selective NO reduction,[49−60] and which mechanism will be discussed in section 5; methanol decomposition,[61,62] phenol steam reforming,[63,64] propene epoxidation,[65] or CO oxidation on a standard composition of a three-way catalyst.[66−68]

Regarding the CO oxidation, the analysis of the $^{12}C/^{13}C$ and $^{16}O/^{18}O$ transient responses indicated that the formation of CO_2 was carried out in two types of active sites, but only a small number influenced the average reaction rate.[66,67]

Table 2. Compilation of Chemical Reactions Studied by SSITKA

reaction/study and catalysts	refs
ammonia synthesis	
Ba promoted Ru/X (X = zeolite)	14
Ru/SiO$_2$	14,16
Cs promoted Ru/MgO	15
Cs,Ba,La promoted Ru/MgO	17
oxidative dehydrogenation	
Rh/SiO$_2$	18
VO$_2$, V$_2$O$_3$, V$_2$O$_5$	19
MoO$_x$/TiO$_2$−SiO$_2$	20
VO$_x$/MCM-41	21
butane isomerization	
sulfated ZrO$_2$	22−25
Pt promoted sulfated ZrO$_2$	24
Al$_2$O$_3$ promoted sulfated ZrO$_2$	25
selective NO reduction	
LaCoO$_3$	49
Pt/SiO$_2$	50−53
Co/ZSM-5	54−58
Pt/Al$_2$O$_3$, Pt/SiO$_2$ promoted by MoO$_3$, Na$_2$O	59
Pt/Al$_2$O$_3$	59,60
methanol decomposition/steam reforming	
Pt,Pd,Rh/CeO$_2$	61
Cu−Mn−O, Cu−Ce−O, Cu-ZnO/Al$_2$O$_3$	62
phenol steam reforming	
Rh,Fe/MgO; Rh,Fe/Mg−Ce−O	
Rh,Fe/Mg−Ce−Zr-O	63,64
propene epoxidation	
Au/Ti-SBA-15	65
automotive exhaust catalysis	
Pt−Pd−Rh/CeO$_2$−ZrO$_2$	66−68
CH$_4$ oxidation	
CaO/Li$_2$TiO$_3$	69
Pd/La$_{1-x}$Sr$_x$MnAl$_{11}$O$_{19}$	70
Pt-X/CeO$_2$ (X = Pr,Gd,Sm)	71
Pt-X/CeO$_2$−ZrO$_2$ (X = Pr, Gd, La)	71
Pd,Pd(PdO),Pt/Al$_2$O$_3$	72−74
CO oxidation	
Au/A$_2$O$_3$, Au/TiO$_2$	75−77
additional oxidation reactions	11,13,78−81
surface acidity	
Zeolites and oxide catalysts	82
N$_2$ adsorption	
LiX (X = zeolite)	83
NaCaX (X = zeolite)	84
KBaLa (X = zeolite)	85

In other cases, the determination of reaction mechanisms becomes more challenging due to the operational factors of the process. The oxidative coupling of methane occurs at very high temperature (573−973 K), and the residence times can be hardly measured by SSITKA at this temperature.[30] Nevertheless, it has been possible to use this technique at a reaction temperature of 918 K.[34] SSITKA gave information about the reaction pathway to generate the coupled products. Ocal and co-workers studied the methane combustion and the effect of NO over hexa-aluminates and Pd-supported hexa-aluminates.[70] The catalysts were tested in the reaction cycle: (1) CH$_4$ + O$_2$, (2) CH$_4$ + O$_2$ + NO, (3) CH$_4$ + O$_2$ at temperatures between 573 and 973 K, and SSITKA was carried out to determine the

surface residence times, site activity, and concentration of the mean species during steps (1) and (2). The results showed that NO_2 is the chain initiator, which enhanced the site activity necessary for the formation of CO_2 and additionally acts as a chain terminator.

SSITKA has been also applied to CH_4 oxidation for a better understanding of the surface dynamics[69] or to evaluate the oxygen mobility in the catalyst.[40,71] Machocki and co-workers reported the methane flameless combustion over a Pd(PdO)/Al_2O_3 catalyst by using the SSITKA method to study the oxygen mobility in the catalyst.[72−74] The results from the switches between $^{16}O_2/Ar/CH_4/He$ and $^{18}O_2/CH_4/He$ indicated that large quantities of oxygen and surface intermediates point to the formation of CO_2 on the palladium surface. The number of active sites increased with temperature due to an increase in the amount of oxygen available from the catalyst. Additionally, Machocki and co-workers found that at the steady-state of methane oxidation on the Pd-based catalyst, there were available short- and long-resided CO_2 molecules on the catalyst surface. The surface residence time of both species decreased with the temperature.[74]

Surface heterogeneity and the effect of promotion have been studied using SSITKA over Ru/SiO_2 catalyst for ammonia synthesis.[16] The catalyst was tested at 674 K, 2 bar, and H_2/N_2 ratio of 3. SSITKA experiments were performed with $^{14}N_2/^{15}N_2$ isotopic switches. The results pointed out that potassium promotion enhanced the reaction rate almost 50 times. This increase was due to the creation of additional super active sites, whereas unpromoted Ru/SiO_2 catalyst has essentially only one type of site. It is the high activity of these new sites which produces the high activity of K promoted Ru for ammonia synthesis. Besides, McClaine and co-workers have studied the ammonia synthesis by SSITKA in order to determine other kinetic parameters, such as TOF and the fractional surface coverage of intermediates.[14,15]

The role of the catalyst composition has been also widely investigated by SSITKA. Support properties, such as acidity or composition, can be crucial for the understanding of the reaction or possible deactivation mechanisms. Kim and co-workers have studied the deactivation of promoted and unpromoted acidic sulfated zirconia (SZ) catalyst in butane isomerization at 423 K.[22−25] The authors discovered that only 1−2% of the total sulfate species appeared to adsorb efficiently reaction intermediates and that the loss of active sites resulted as the main reason for catalyst deactivation. It appears that the deactivation of the active sites was the main reason for the fast deactivation, less than or equal to 100 min on stream. The deactivation mechanism of the active sites was associated with the possible sulfur reduction and coke/oligomer formation on the catalyst surface.[23] Regarding the role of promoters, SZ doped by Al_2O_3 showed a substantial increase in the concentration of surface intermediates, which can explain the approximate 30% increase in catalytic performance at 523 K.[25] SZ doped by Pt and the addition of hydrogen to the reaction mixture showed a great decrease in the deactivation during isomerization.[24] In order to improve the activity or the stability of the catalyst, platinum requires the presence of additional hydrogen in the feed. The activity and stability of the catalyst was improved, despite that the average reaction rate decreased slightly, when both H_2 addition and Pt promotion were used at 523 K as a result of an increase in the active surface intermediates leading to the product.

Another feature of the support that has been evaluated by SSITKA is the physisorption capability. Bajusz and co-workers reported the study of N_2 adsorption behavior in a LiX zeolite.[83] Nitrogen adsorption isotherms at different partial pressures of N_2 were measured at temperatures between 303 and 338 K using isotopic switches between $^{14}N_2/^{15}N_2$. The results showed that the amount of N_2 adsorbed obtained per total Li cation (between 0.01 and 0.06 molecules/cation) are in good agreement with the data collected using other techniques. SSITKA also allows comparing the adsorption behavior of gas mixtures—that is, O_2 and N_2.[84]

In summary, the SSITKA technique can be applied to a wide range of different reactions, and it is not only a valuable technique to calculate kinetic parameters in order to elucidate reaction pathways. Additionally, it also enables the possibility to study the properties of the catalyst, the site heterogeneity, or the effect of its composition in the reaction mechanism. Advanced calculation and modeling methods provide a way to obtain more information about kinetic parameters such as reactivity distribution and, in some cases, side processes such as readsorption reactions.

3. STUDY OF FISCHER−TROPSCH SYNTHESIS BY SSITKA

The catalytic production of hydrocarbons from synthesis gas (mixture of H_2 + CO), universally named Fischer−Tropsch (FT) synthesis, is considered an outstanding industrial process because it allows the transformation of different carbon resources into valuable chemicals or liquid fuels. A wide variety of products can be obtained depending on different factors, such as catalyst composition, reaction conditions, or experimental parameters (i.e., reactor design).[86−89] The FT mechanism is known to be a polymerization-like reaction with a high number of intermediate steps involved, and it is strongly dependent on catalyst composition. Thus, due to the complexity of the process, several suggestions for the reaction mechanism have been proposed to explain the different selectivity obtained, which depends on the polymerization chain growth probability.[87,90−93] The identification of the chain initiator and the study of its propagation is the key for understanding and predicting the product selectivity as well as for the design of the catalyst.

Within the different proposed mechanisms, there is only limited understanding of the quantity, reactivity, and chemical identity of the participating surface species.[94] For this reason, the CO hydrogenation has been the most investigated reaction by SSITKA aiming at a better understanding of this complex reaction mechanism, although still nowadays there are many aspects that are still in debate.

3.1. Effect of Catalyst Properties and Operating Conditions. Many authors have carried out their research on the study of the effect of different parameters, for instance, catalyst properties (metal identity, promoters, supports, and metal particle size) and operating conditions (H_2 and CO partial pressures, temperature, activation method, water) on CO conversion and product distribution using SSITKA to elucidate their effects on catalytic performance in terms of the number of the intermediates, the site reactivity or other kinetic parameters. Co- or Fe-based catalysts have been studied extensively in Fischer−Tropsch synthesis, but also the reaction has been carried out on noble metal such as, Ru, Pt, and Rd (Table 3).

3.1.1. Effects of Catalyst Properties. Among all the parameters studied, promoter effects were mostly investigated by SSITKA. For Co-based catalysts, the promoters Re, Pt, Ru, La, and alkali metal were studied. Re,[95] Pt,[96,97] Ru[98] were reported to significantly increase catalyst activity and Re could slightly enhance C_{5+} selectivity.[28,95−100] Promotion facilitates the reduction of cobalt atoms and increases the number of metallic cobalt exposed to the reaction feed, resulting in an increase in the reaction rates. SSITKA with carbon tracing was carried out to evaluate both number of active intermediates and its intrinsic reactivity during the Fischer−Tropsch synthesis. SSITKA studies reveal that the addition of nobel metals promotes the concentration of active surface intermediates leading to CH_4, whereas no substantial influence was detected by addition of rhenium or platinum. Oxide promoter La[101−103] and MnO_2[104,105] were reported to mainly increase higher hydrocarbon selectivity. Small amounts of La^{3+} increased activity, whereas excess La^{3+} caused a decrease in activity. SSITKA studies showed that the observed changes in activity are due to changes in the overall amount of intermediates leading to methane (N_{CHx}) but not due to changes in its reactivity. However, MnO_2 promotion raises the residence time and site coverage of N_{CHx}. In addition, higher N_{CHx} coverage affects the selectivity toward C_{5+} and methane compounds. Higher coverage of N_{CHx} intermediates could lead to a high chain growth probability, which causes an increase in selectivity toward C_{5+} hydrocarbons and a decrease in selectivity to methane.[104]

Iron-based catalysts are frequently promoted by adding alkali metals (Li, Na, K) in ppm level, whereas small amounts could significantly decrease catalytic activity for Co-based catalyst.[106−108] Carbon selectivity to CH_4 decreased with increasing alkali loading, while CO_2 and C_{5+} hydrocarbon selectivities increased. SSITKA study on 1% and 2% Na promoted Co catalysts showed that the presence of sodium decreases substantially the amount and reactivity of surface intermediates leading to methane, probably due to a lower H coverage, electronic effects, and site blocking by sodium atoms.[106]

K and Cu are most commonly used promoters for Fe-based catalysts; K enhances higher hydrocarbon selectivity, while Cu mainly enhances the reduction of Fe. Addition of potassium to iron or Mn-promoted iron catalysts has different effects depending on the concentration of potassium, regardless of the presence of Mn. Although low K concentrations can enhance the catalytic activity, the percentage of light olefins (C_2−C_4 fraction) and chain growth probability (α), the excess of K can reduce the catalytic activity.[109] The enhancement in catalytic activity was related to an increase in the number of N_{CHx} intermediates leading to the formation of hydrocarbons. The methane formation over (un)promoted iron catalysts with K were studied by dosing CO in hydrogen in another study.[110] The results suggested that the presence of potassium establishes a new and slower reaction route toward methane formation, while the reaction route toward higher hydrocarbons remains unchanged.

The catalytic activity in the Fischer−Tropsch and the water−gas shift (WGS) reactions may also be raised by adding other transition metals (Cr, Mn, Mo, Ta, V, W, Zr) to Fe and Cu (all except W). The highest increase was achieved by Cr-, Mn- and Zr-promotion, despite that it did not affect hydrocarbon selectivity.[111] The enhancement in the catalytic activity has been related to an increase in the number of intermediates leading to hydrocarbons.[112−115]

Noble metals are also active for CO hydrogenation; however, the price limits their use at an industrial scale. Alkali promotion has been studied on noble metals (Ru, Pt, Pd) for FT synthesis.[116] SSITKA experiments using $^{12}C/^{13}C$ switches were performed to study the effects of potassium on the methane-producing sites during CO hydrogenation over Ru/SiO_2 catalysts with K-promotion loadings (K/Ru atom) up to 0.2. The SSITKA results indicated that carbidic carbon species evolved into methane via two different pathways: a high-reactivity ($C_{1\alpha}$) and a low-reactivity ($C_{1\beta}$) route.[43] High concentration of potassium promoter decreases the abundance and the intrinsic activity of both pools, affecting $C_{1\alpha}$ to a greater extent. The detriment effect may be caused by changes in carbon−metal interaction due to the presence of potassium. The promotion may be able to strengthen this interaction, making the hydrogenation step more difficult. Methanation was investigated on a 4.5 wt % Pt/SiO_2 promoted with different amount of K^+ (K^+/Pt = 0, 0.1, 0.2) for two different temperature ranges (503−552 K and 573−665 K).[117] Kinetic studies combined with SSITKA suggest that K^+ serve as a rate promoter at low reaction temperatures, whereas its only effective function is site blockage at higher temperatures. Li promotion is known to increase the methanol synthesis reaction rate on Pd. The mechanism of Li promotion of Pd/SiO_2 at 483−563 K and 1.8 atm was studied using SSITKA with $^{12}C/^{13}C$ isotopic switches to reveal the consequences of Li addition on the methanol-producing sites during the first 10 min of reaction.[118,119] The results pointed out that Li increased the active surface intermediates concentration, most probably due to a higher number of surface sites or an increase in the site coverage of the active intermediates on the surface. However, the calculation of the methanol formation rate constant (k_{MeOH}) showed a lower value for the promoted catalyst. Nevertheless, the overall effect is that Li promotion enhances the catalytic activity because the changes in the concentration of active sites is more significant than the changes in the rate constant values.

Support modification is another way to tune the catalytic activity and selectivity. The addition of zirconia and zinc to the alumina on supported cobalt catalysts has been studied under CO hydrogenation.[120−124] Zirconia promotion has positive effects in the catalytic performance, leading to an increase in both catalytic activity and selectivity to hydrocarbons. These effects may be due to an enhancement of Co reducibility by the presence of Zr which could inhibit Co aluminates formation over the surface. SSITKA results have demonstrated that the main effect of Zr on the catalysts is the increase in the number of active intermediates and active Co surface sites, whereas the changes in intrinsic activity were negligible. Impregnation of Co−Re catalyst with Zn showed a strong and negative loading-dependence effect on catalytic performance in terms of activity and selectivity, whereas the addition of Zn to the support followed by calcination at 1173 K and impregnation with Co−Re had negligible impact on the selectivity toward high hydrocarbons (C_{5+}).[124] The detrimental effects of Zn have been ascribed to similar effects observed after the addition of alkalines reported in the literature.[125,126] SSITKA tests pointed out that the presence of Zn causes both increase in the residence time of intermediates leading to methane and a decrease in selectivity toward methane. Otherwise, Zn has no effect on the concentration of adsorbed carbon monoxide (N_{co}).[123]

Table 3. Role of Different Parameters in Fischer−Tropsch evaluated by SSITKA

parameters	comments	refs
promoters		
Co−La, Pt, Ru, Re, Alkali(Na,K, Li), MnO$_2$, Cu	Pt, Ru, Re increase activity, slightly enhance selectivity for Re, increase number of intermediates	28,95−100
	Na, K, Li decrease activity, enhance C$_{5+}$ selectivity, decrease in both intermediates and intrinsic activity	106−108
	La, MnO$_2$ causing increase or decrease intermediates, may cause change in intrinsic activities	101−105
	Cu enhances the selectivity toward alcohols but reduces CO conversion	153
Fe−K,Mn,Cr,Zr	increase active surface intermediates leading to hydrocarbons, K may change the methane formation routes	109−115
Ru−K	decrease the amount and reactivity of two carbidic pools leading to methane	116
Pt−K	K$^+$ serve as a rate promoter at low reaction temperatures while its only effective function is site blockage at higher temperatures	117
Pd−Li	increase active surface intermediates, slightly decrease intrinsic activity	118,119
support modification		
Co−Zr, Zn, alumina phase, mesoporous alumina, mesoporous silica	Zr increase active surface intermediates, not influence intrinsic activity	120−122
	Zn decreases intrinsic activity	123−126
	alumina phase and morphology modify surface intermediates, do not change intrinsic activity	127,128
particle size		
Co	higher coverage of irreversibly bonded CO, lower amount of active surface intermediates, lower or constant intrinsic activity	130,131,135,136
Ru	lower amount of active surface intermediates, constant intrinsic activity, increased CO residence time	129,132
process conditions		
temperature	increase intrinsic activity ($1/\tau_{CH4}$)	137
H$_2$ partial pressure	increase surface H concentration, increase intrinsic activity($1/\tau_{CH4}$), may change surface intermediates(N$_{CH4}$)	139,143
H$_2$/CO ratio	affect the intrinsic activity (τ_{CH4}) slightly	137
water[154]	small amount of water increase activity by increasing amount of surface carbon	142
	excess amount cause deactivation due to decreased active surface intermediates	140,141
activation	increase intrinsic activity ($1/\tau_{CH4}$)	152

The characteristics of alumina, such as crystalline phase and pore size have an impact on the cobalt activity and selectivity.[127] SSITKA experiments switching between ^{12}C/^{13}C showed an increase in the number of intermediates leading to methane upon catalysts with medium pore size compared to catalysts with smaller pore size. Higher number of intermediates was also found in samples with δ- and α-Al$_2$O$_3$ phases compared to γ- and θ-Al$_2$O$_3$. The same trend observed in the amount of active intermediates is also followed in terms of selectivity toward C$_{5+}$. α-Al$_2$O$_3$ showed the highest selectivity to C$_{5+}$; however, it suffers from low cobalt dispersion due to low surface area. In order to take advantage of the catalytic performance offered by α-Al$_2$O$_3$, a new macroporous structured (MPS-Al$_2$O$_3$) support was synthesized from α-Al$_2$O$_3$ nano-particles to improve the supported cobalt dispersion.[128] The results obtained with this new support combine the benefits obtained of α-Al$_2$O$_3$ and γ-Al$_2$O$_3$ as supports, displaying similar catalytic performance compared to conventional Co/γ-Al$_2$O$_3$ and Co/α-Al$_2$O$_3$ catalysts, respectively. The kinetic parameters such as intrinsic rate constant and site coverage of intermediates leading to methane remains unchanged as Co/α-Al$_2$O$_3$, whereas the number of active intermediates has increased substantially due to better cobalt dispersion on MPS-Al$_2$O$_3$. Similarly, mesoporous MCM-41 supported cobalt catalysts have higher reaction rate compared to silica supported ones. These results are ascribed to a larger amount of surface intermediates but not the result of changes in their intrinsic activity.

The SSITKA technique has been successfully applied for understanding particle size effect on the FT synthesis.[129−132] It

has been extensively accepted that there is no significant change in the reaction rate for cobalt particle sizes larger than 10 nm.[133] Catalysts containing Co particles below 10 nm showed higher methane selectivity and an overall decrease in catalytic activity.[130,131,134−136] In the case of cobalt supported on carbon material with smaller Co particles (<6 nm), SSITKA reveals an increase in the residence times of reversibly bonded CH$_x$ and OH$_x$ intermediates, while the residence time of adsorbed carbon monoxide decreased. In terms of coverage of the reactants, small Co particles showed higher coverage of irreversibly bonded CO, a fact that was related to an increase in the number of low-coordinated sites on the surface. Conversely, this catalyst showed a higher hydrogen coverage that increased the selectivity toward methane. In addition, it has been observed that small Co particles showed lower turnover frequency (TOF) values. This phenomenon has been related to a lower intrinsic activity of the small Co terraces and to a blockage of corner sites. The study on cobalt catalysts supported on alumina showed a decrease of surface intermediates without changing the intrinsic activity (τ_M) on different sized particles.[130] Both studies pointed to the fact that a larger fraction of the cobalt surface was blocked when particle size is smaller than 6−8 nm at reaction conditions. The particle size effect has also been reported on Ru/γ-Al$_2$O$_3$ catalyst from a size range of 4−23 nm.[134] Ru clusters <10 nm showed a decrease in CO residence time as the cluster size increases up to 10 nm. These results have been related to a partial blockage of active sites originated by a stronger CO adsorption on the clusters.

The effects of rhenium promotion, cobalt loading, or different support composition of the support have been studied by SSITKA regarding methane selectivity and reaction rate. The results over the catalysts tested showed negligible differences in the surface residence time of intermediates leading to methane, which means the intrinsic activity is independent of promotion, cobalt loading, and support. This is consistent with what has been discussed above. The major changes of activity and selectivity are due to the change in abundance of surface intermediates (N_{CH4}) instead of an impact on intrinsic activity (τ_{CH4}). Alkali promoter (Na, K, Li) or oxide promoter (Mn, Zn, La) might influence intrinsic activity (τ_{CH4}) trough modification of the interaction of CO with cobalt.

3.1.2. Effects of Operating Conditions. Operating conditions may have a significant impact on the catalytic performance. The effects of H_2 and water pressure, temperature, and H_2/CO ratio were investigated by SSITKA.[137−142] The study on Co/γ-Al$_2$O$_3$ and CoRe/γ-Al$_2$O$_3$ catalysts showed that changes in CO partial pressure or operating conditions, such as temperature or space velocity, have no significant influence in CO adsorption. The intrinsic activity (τ_{CH4}) may be slightly affected by changes in space velocity, H_2/CO ratio, and temperature, whereas the total or partial pressures of the reactants have a tenuous effect.[137] It has been also pointed out that changes in operating conditions, such as temperature, total pressure, H_2/CO ratio or H_2, CO partial pressures have no significant influence on the concentration and site coverage of surface intermediates. Methane selectivity showed a remarkable dependence toward operating conditions, indicating that methane selectivity is being influenced not only by its surface precursors but also by operating conditions. The relative coverage of hydrogen can be estimated from SSITKA parameters and increases at higher H_2 partial pressure.[139] Since higher hydrogen coverage enhances the hydrogenation of the surface carbon, this is suggested to explain increase in the surface coverage of methane intermediates (N_M) with H_2 partial pressure. N_M showed a complex dependency on H_2 partial pressure, temperature, and deactivation.[138] The average surface residence time of the methane intermediates (τ_M) decreased accordingly with increasing H_2 partial pressure because the pseudo-first-order rate constant, defined as the inverse of the surface residence time ($1/\tau_M$), includes the hydrogen surface concentration.[139,143]

Water is reported to enhance selectivity of higher hydrocarbons (C_{5+}). The effect on the FT activity is very complicated and depends on various factors, such as water partial pressure and catalyst support type.[140−142,144−152] Positive effect, negative effect, and no effect have all been reported. The effect of water on the FT synthesis over alumina-supported cobalt catalysts has been studied using isotopic transient kinetic methods (SSITKA) in combination with steady-state measurements. The catalyst was tested before and after water treatment, and water addition decreased the total number of active surface sites without changing its intrinsic activity.[140,141] On a Co−Re catalyst, it was revealed that water promotes the formation and deposition of monomeric carbon species on the catalytic surface,[142] due to the enhancement of CO dissociation without promoting the formation of hydrocarbons. These results give an explanation to the lower methane and higher hydrocarbons selectivities achieved under the presence of high amounts of water.

As a summary, Table 3 contains a compilation of the effects of different parameters evaluated in Fischer−Tropsch reaction mechanism by SSITKA.

3.2. Study of Reaction Mechanisms. SSITKA analysis helps to determine some kinetic parameters of the intermediates, but it is not possible to describe the complete reaction mechanism. Due to the complexity of Fischer−Tropsch synthesis, it is very common to set the reaction conditions to favor the formation of methane by increasing the partial pressure of hydrogen (also called methanation conditions) to simplify the reaction mechanism and develop an easy way to study the kinetic parameters.

In order to study the Fischer−Tropsch process under industrial conditions and, thus, obtain a complex product distribution, it is necessary to include other methods to determine the reaction intermediates and the kinetic parameters of the reaction pattern.[155−160] To achieve this aim, many authors have completed the SSITKA analysis with multiproduct analysis,[161−164] theoretical modeling,[165−168] density functional theory (DFT) methods, isotopic tracing,[26,169,170] or use of probe molecules,[171] among others.[2,3] Besides, it is possible to find in the literature various studies of chemical reactions different from Fischer−Tropsch that have been studied combining SSITKA analysis with theoretical modeling.[13,44,53,55,69,81,158,172−177]

The multicomponent SSITKA is a methodology used previously by Stockwell and co-workers[178] and more recently by Goodwin Jr. and co-workers[161−164] to study the kinetics of CO hydrogenation. Different samples of the multiple products formed during CO hydrogenation are collected, separated by gas chromatography, and then the C_{2+} products are converted to CH_4 through a hydrogenation reactor prior to their admission to the mass spectrometer. The main advantage of this method is that it is possible to construct the isotopic transients for the various products and determine their surface parameters without overlapping the signals of the different products due to MS fragmentation. This methodology permits the researcher to compare and figure out on which active sites the different products appear to be formed and determine whether similar products are formed through the same active site pattern.

New approaches for unravelling complex reaction mechanisms have been achieved combining the integration of transient and steady-state kinetic modeling, experimental, and/or DFT investigations. To date, the reaction mechanisms reported in the literature are not able to describe the full distribution of Fischer−Tropsch possible products. Kinetic equations proposed for this process are based on mechanisms with postulated rate-determining steps or have been developed empirically. The FT reaction mechanism has been mainly studied in combination with CSTR reactor modeling under methanation conditions[27,47,48,178] and only a few investigations deal with PFR modeling, adding C−C coupling reaction rates, surface concentrations or included possible adsorption−desorption of the intermediates.[27,45−47]

Schouten and co-workers have combined experimental data and computational modeling to identify and discriminate between different mechanistic models for the Fischer−Tropsch synthesis.[27,45,46,48,179] First, they considered only the methanation reaction,[27] and then they expanded the modeling including C−C bond coupling reaction by introducing the formation of ethane. Experimentally, they have analyzed the transient response of the C_{2+} compounds by GC-MS product analysis,

which allows the detection of non-, partial-, and fully labeled compounds. This method allowed them to propose a mechanism where C_s and CH_s were the active C_1 species and both participate in chain initiation to form reactive C_2 species, such as C_sCH_s. This model can be extended to the formation of C_3 species but there are some limitations in detection of C_3 partially labeled transients, and thus, it is difficult to optimize the rate constants for C_3 compounds. Figure 6 showed a summary of reaction routes in the Fischer–Tropsch process.[48]

Holmen and co-workers have included DFT investigations of kinetic isotopic effects in the experimental data and modeling in order to determine the equilibrium constants of H_2 and CO adsorption and a detailed collection of surface species, including their concentrations and reactivity under methanation conditions over carbon nanotubes.[47] The results showed that the CO activation route goes by a hydrogen-assisted CO dissociation, and as a consequence, two different carbon intermediates leading to two different reaction pathways for methane formation were found.

4. APPLICATIONS OF SSITKA IN REACTIONS FOR FUEL CELLS AND PHOTOCATALYSIS

4.1. Reactions for Fuel Cells Studied by SSITKA. Fuel cells are considered a potential technology due to the wide range of possible applications, for example, as a substitute of internal combustion engines in vehicles or their use as electric power generators. Proton Exchange Membrane Fuel Cells (PEMFCs) can transform a source of hydrogen and oxygen into energy and water as a byproduct. The typical hydrogen used in fuel cell technologies contains CO and CO_2 in a concentration level around 1% (10 000 ppm) because it is traditionally produced from the partial oxidation or the steam reforming of hydrocarbons. A variety of further purification steps must be carried out since removing CO from the stream is remarkably important for operating the fuel cells efficiently. It is well-known that the presence of CO at ppm levels can poison the platinum anode by adsorbing firmly on the platinum surface and blocking the sites for hydrogen oxidation. For this reason, the level of CO in hydrogen must be below 10 ppm to be used in fuel cells.

SSITKA experiments are very effective to evaluate and compare the H_2 and CO competitive adsorption on anode surface using the isotopic exchange between ^{13}CO and ^{12}CO. Sirijaruphan, Goodwin Jr., and co-workers have demonstrated the utilization of metal foams in the selective oxidation of CO using Au, Pt, and Fe-promoted platinum catalysts.[11,180,181] The results in surface coverage and CO_2 selectivity have been compared to the typical powder catalysts. Figure 7 shows SSITKA results (rate constant, surface intermediates, and surface CO concentrations) for both powdered and foam-based Pt catalysts with different pore size.[180] The foam-based and the powdered catalysts with analogous composition showed similar CO oxidation activity. A low total amount of CO adsorbed during reaction, higher CO_2 selectivity, and higher pseudo-first-order rate constant were observed in the foam-based catalyst compared to the powdered catalyst due to iron impurities present in the washcoat coming possibly from the metal foam. No significant differences were found in the concentration of active surface intermediates for both types of catalysts. All the catalysts tested showed a great initial performance in terms of activity and selectivity during the first 30 min on stream followed by severe deactivation.[11] SSITKA analysis pointed out
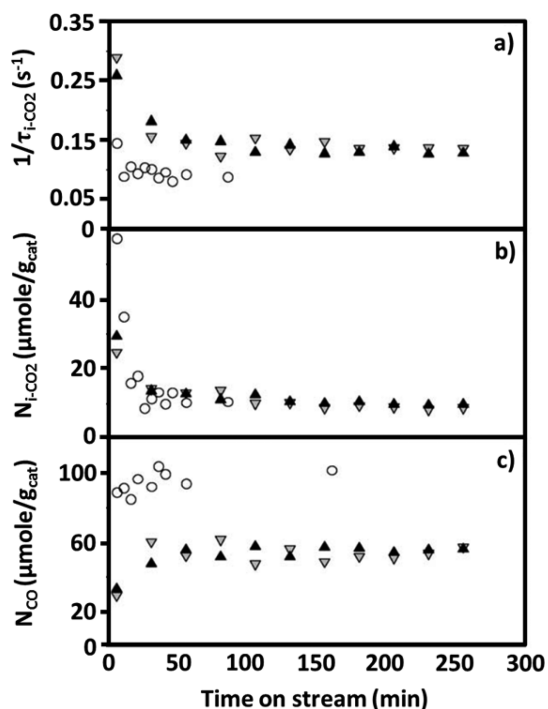

Figure 7. SSITKA results: (a) average pseudo-first-order rate constant; (b) concentration of surface CO_2 intermediates; (c) total concentration of surface CO for the powdered Pt (O) and foam-based Pt catalysts (gray $\triangledown$ = 405Pt, $\blacktriangle$ = 505Pt). (Reproduced from ref 180. Copyright 2005, Elsevier.)

that the deactivation was mainly caused by a decrease in the amount of surface CO_2 intermediates.

Davies and co-workers have studied the relevant adsorption and desorption rate constants of the processes that occur in the anode of a PEM fuel cell over platinum and platinum–ruthenium catalysts.[182–184] SSITKA experiments have been carried out using $^{13}CO/^{12}CO$ switches to study the H_2 and CO competitive adsorption on commercial Pt and PtRu catalysts. The results showed that the addition of ruthenium as a second metal increases the tolerance toward CO adsorption on the anode.[185] This promotion may be explained by three different proposed mechanisms: the bifunctional effect, the ligand effect, and the detoxification mechanism. A detailed description of the different mechanisms can be found in the literature.[184,186–188] The authors have compared these results with those obtained using 100 ppm of CO in H_2. The main conclusions of this work indicated that at high concentration of CO there is no significant difference in the rate of exchange on Pt and PtRu. At concentrations around 100 ppm, the competition between hydrogen and CO arises and the exchange rate on PtRu surface is lowered compared to the exchange rate on Pt. This phenomenon can be explained due to lower equilibrium coverage for CO on PtRu catalyst, which enhances the oxidation of hydrogen. The balance between the rate of exchange and equilibrium coverage becomes a key feature to elucidate the main mechanism for CO tolerance.

4.2. Use of SSITKA in Photocatalysis. The removal of hazardous chemicals has become a relevant concern because of the considerable increase in environmental pollution due to the exponential growth of population and the increase of industrial activities. Photocatalysis arises as an auxiliary process to standard techniques to convert hazardous wastes, such as filtration, anaerobic digestion, or physicochemical treatments.
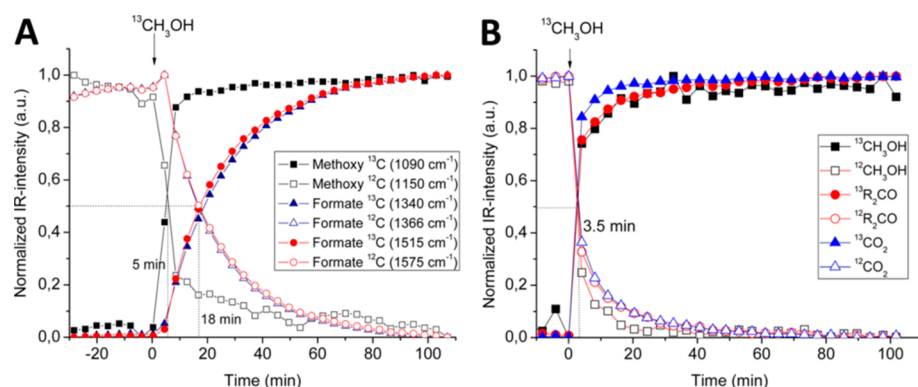
Figure 8. IR band intensities versus time (A) for adsorbed species on TiO$_2$−P25 and (B) for final products in the gas phase. (Reproduced from ref 189. Copyright 2013, American Chemical Society.)

Heterogeneous photocatalysis is nowadays a well-known process for the oxidation of pollutants in air but is still challenging due to the complexity of studying heterogeneous catalysts in the gas phase compared to liquid phase.

The operando infrared (IR) technique applied to heterogeneous catalysis has been developed recently to study some processes for air purification. This is a powerful technique to establish the composition of the intermediates that are involved in the process and propose a reaction mechanism. Unfortunately, it is not possible to study the kinetic parameters to validate the air purification mechanism. For these reasons, it has been further investigated by the use of the SSITKA technique in combination with an operando analysis to elucidate the nature of the main intermediates and the determination of the kinetic parameters. El-Roz and co-workers have applied this integrated technique in the photocatalytic oxidation of methanol.[189] This work investigates the kinetics of the reaction mechanism in the study of a new photocatalyst (hierarchical TiO$_2$, named TiO$_2$-L) in air purification from MeOH as standard for volatile organic compounds (VOCs). The performance of this new photocatalyst has been compared to the performance obtained by commercial TiO$_2$, named TiO$_2$−P25. SSITKA switches between $^{12}CH_3OH$/$^{13}CH_3OH$ coupled with an operando IR analysis system exhibited outstanding results in the qualitative determination of intermediates in methanol oxidation.

This new operando spectroscopic technique showed an advancement in studying the photocatalytic activity and could also describe the role of the surface species in the reaction mechanism. In Figure 8, the changes in IR band intensities for adsorbed species and final products on TiO$_2$−P25 after the switch $^{13}CH_3OH$/$^{12}CH_3OH$ are depicted. This study allowed establishing relationships between intermediates and final products. Formates generated on TiO$_2$-L showed higher stability than on TiO$_2$−P25. Only a small fraction of the overall amount of formate species on the surface of the catalyst is involved in the main reaction mechanism, whereas the other formate species are merely spectators. During SSITKA experiments, the shift rates between methoxy species and final products were comparable on both photocatalysts (as seen in Figure 8), denoting methoxy species as the main intermediates in methanol photo-oxidation.

5. SSITKA COUPLED WITH SPECTROSCOPIC TECHNIQUES

One of the limitations of the SSITKA technique is that it is unable to determine the composition of intermediate species. This technique allows identifying abundance of intermediates and their kinetic parameters, but it is not possible to determine the composition of the adsorbed intermediates involved in the reaction mechanism. Otherwise, Infrared (IR) spectroscopy is commonly used to study the interaction between adsorbed species and heterogeneous catalytic surfaces,[190] but the experiments are usually carried out under conditions that are not suitable to determine kinetic parameters.

The combination of in situ/operando spectroscopic data and kinetics was first introduced by Dalziel et al. in 1957[191] and Tamaru et al. in the 1960s.[192,193] The studies of Tamaru and co-workers were the first tries to establish a correlation between the reactivity of surface species and reaction rates measured in the water−gas shift reaction over catalysts containing metal oxides. Transmission IR spectroscopy allows the direct observation of adsorbed species under reaction conditions. Coupling in situ IR with SSITKA may supply valuable information on the surface coverage of IR observable species under reaction conditions and the combination of both techniques offers the possibility to discriminate between main intermediates and adsorbed species that do not participate directly in the reaction mechanism, commonly named spectators. The collection of infrared spectroscopic data and kinetic measurements can grant us the ability to link a particular surface intermediate to a given reaction product.[194]

The main difficulty of the combination of these techniques is the construction of the reaction cell, because they have to be designed and built specifically to carry out both measurements under the desired reaction conditions. It must be pointed out that the reaction chamber used by Tamaru and co-workers[192,193] was a dual-bed cell—one section needs a small amount of sample (around 300 mg) to carry out transmission IR measurements and a second section containing around 10 g of catalyst to perform the transient kinetics measurements, because an assessable conversion level is required. The utilization of a dual cell implies the challenge that each section depends on different experimental parameters and is more complicated to ensure steady-state conditions in both parts.

Chuang and co-workers were the first to couple both techniques using a single bed reactor during the 1990s.[195−198] This is a very valuable improvement and can be used to elucidate the role of the surface species detected on catalytic
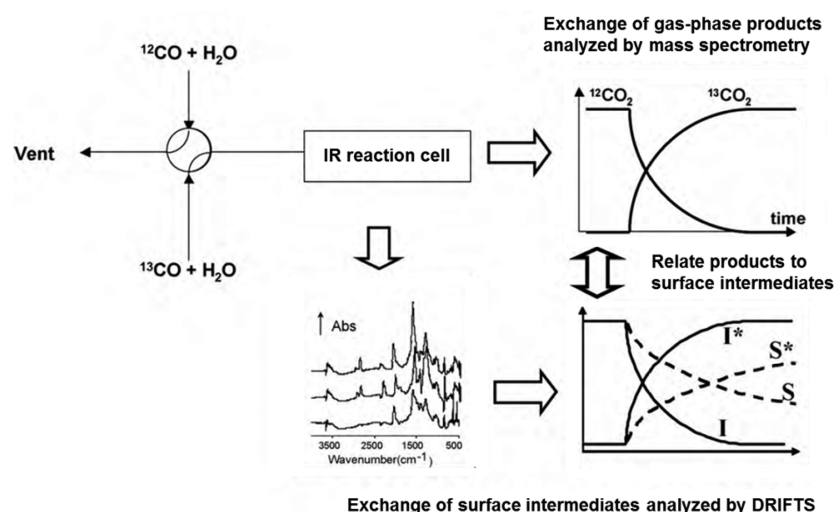
Figure 9. Scheme of the IR-MS-SSITKA system for the operando investigation of catalytic reactions. True reaction and minor intermediates are denoted as I and S respectively. (Adapted from 194. Copyright 2010, Elsevier.)

surfaces under reaction conditions. A scheme of the system is displayed in Figure 9, extracted from Meunier's review.[194]

The discrimination between active and spectator species can be achieved by comparing the isotopic exchange rate of the surface species measured by operando IR to the exchange rate of the species in the gas phase measured by MS. Surface species can only contribute to the main reaction pathway if the isotope exchange is as fast as the exchange of products in the reactor outlet. Minor reaction intermediates and spectator species are detected by slower isotopic exchange or no exchange, respectively.[194]

The SSITKA technique has been also coupled to other infrared techniques, such as DRIFT (Diffuse Reflectance Infrared Fourier Transform) spectroscopy. Goguet and co-workers were the first group to report an isotopic transient study testing a DRIFTS cell as a single bed reactor.[199] A scheme of the reactor design can be found in the review of Yang and co-workers.[200] The main difference between DRIFTS and transmission mode is that only a minor portion of the sample is being tested, and therefore, less resolution is obtained in reflectance mode. Besides, concentration gradients may occur because of nonzero conversion over the packed bed as well as the possibility of temperature gradients within the sample. The main studies using the combination of SSITKA and DRIFTS techniques are focused on the reactivity of surface species under reaction conditions. Although this technique has been mainly applied in a qualitative point of view, it has been proved that DRIFTS can be an accurate quantitative tool for operando studies if an appropriate calibration relating band intensity to the concentration of the species adsorbed on the catalyst is procured.

Table 4 compiles in chronological order the basic processes that have been studied up to date by coupling SSITKA and IR techniques (both transmission and DRIFT) spectroscopies. Even though there is a wide range of different reactions studied, the main focus is common, as mentioned before: the coupling of these techniques can procure information about the site coverage of IR observable species and can potentially discriminate between real and spectator intermediates.

In the 1990s, the spectrokinetic studies were focused on oxidation,[207−212] methanation,[197,241,242] and hydroformylation[195,196,244−246] reactions of small molecules. The exper-

imental limitations and the utilization of dual cells provoked that only a limited group of catalytic reactions could be carried out. At the beginning of the 2000s, the studies were centered on selective reduction processes,[233−240,248,249] which meant that these techniques helped to improve the understanding of the reaction mechanism of automotive catalysts. Because the SSITKA technique was coupled to DRIFT spectroscopy for the first time in 2004[199] and because of the improvements achieved in the reactor design, the studies started to investigate the water−gas shift (WGS) reaction in its reverse−forward directions.[173,199,203,213−217,219−232] In recent years, other applications can be found in the literature; for example, in the work of Theologides and co-workers,[243] spectrokinetic techniques have been adapted to study the hydrogenation mechanism of nitrates in water media, as well as in photocatalytic applications, as explained in section 4.2.

As discussed in section 3, the reaction mechanism and kinetics of methanation have been intensively studied by SSITKA, and the surface coverage of CO and the surface pool leading to methane formation were measured on different catalysts and different conditions. In situ IR spectroscopy combined with SSITKA was found to be an effective tool to identify the nature of the surface pools leading to methane formation. The results revealed that the reaction mechanism depends on the catalysts used. Different CO species bonded to the surface, such as linear and bridged molecules, were found on Ni/Al_2O_3,[201] Ni/SiO_2[29] and Rh/SiO_2.[202] The results showed that CO dissociation mechanism prevailed over hydrogen-assisted CO activation because no reactive H−C−O species were detected on these catalysts. The nature of the CH_x pool could be further investigated using these combined techniques. No CH was found on Ni/Al_2O_3[201] which suggested that "x" in CH_x is close to zero. Surface carbon (C*) is dominating in the surface pool on both Ni/Al_2O_3[201] and Ni/SiO_2[29], and a single rate-determining step was found. The overall methanation rate is regulated by the competitive reactions of carbon formation and hydrogenation over the catalytic surface.[201] However, in situ IR spectra and transient responses revealed that adsorbed CO can be exchanged easily with gaseous CO and that the hydrogenation of CH_x intermediate is the rate-determining step under steady-state conditions on Rh/SiO_2.[202] Compartment modeling and site

Table 4. Compilation of the Studies Carried out Coupling SSITKA and Spectroscopic Techniques

reaction and catalyst	refs
CO hydrogenation	
Ni/Al$_2$O$_3$	201
Rh, Ni, Cu, Ru/SiO$_2$	29,202,203
Co/MgO	204
Ru/zeolite, Ru/Al$_2$O$_3$	205,206
oxidative catalysis	
review of different reactions	207
CO oxidation over Pt	208
DME oxidation over MoO$_x$/Al$_2$O$_3$	209
CO oxidation over Pd/CeO$_2$–ZrO$_2$–Al$_2$O$_3$	210
methanol oxidation over Au/CeO$_2$	211
carbonylation of MeOH over Cu/Y	212
water-gas-shift (WGS)	
Pt/CeO$_2$	173,199,213–218
Au/Ce(La)O$_2$	219
Au/CeZrO$_4$	217,220
Pt/ZrO$_2$	221
Pt, Pd, Rh/Al$_2$O$_3$	222,223
Pt over CeO$_2$–MgO, Ce$_x$Zr$_{1-x}$O$_2$, CeO$_2$–La$_2$O$_3$ or CeO$_2$–TiO$_2$	224–228
Pt/TiO$_2$	229
Pt/ThO$_2$	228
Au/TiO$_2$	230,231
CeO$_2$/CuO	232
selective catalytic reduction	
Pt/SiO$_2$	233
Pt/La–Ce–Mn–O	233
Pd/Al$_2$O$_3$	234
M/Co$_3$O$_4$ (M = alkali)	234,235
Ca/La$_2$O$_3$	236
Fe–Pd–Rh/CeO$_2$–Al$_2$O$_3$	237
Pt/MgO-CeO$_2$	238,239
Fe/HBEA	240
methane reforming	
Rh/Al$_2$O$_3$	197,241
(Pt, Ru, Ni, Ni–Ru)/L$_x$(Ce$_{0.5}$Zr$_{0.5}$)$_{1-x}$O$_2$ L = Pr,Sm,Y	242
hydrogenation of nitrates in water	
Pd–Cu/γ-Al$_2$O$_3$, Pd–Cu/TiO$_2$–Al$_2$O$_3$	243
ethylene hydroformylation	
Rh, Mn–Rh, Ce-Rh/SiO$_2$	33,195,196,244–246
n-butane isomerization	
sulfated zirconia	247

distribution analysis of the transient responses show that CH$_x$ is hydrogenated to CH$_4$ via a bimodal distribution of the rate constant, where CO dissociation was detected as the rate-determining step and linear CO depletes faster than bridged CO.[202] The power of the combined techniques (temperature-screening and kinetic measurements, DRIFTS and SSITKA) in mechanistic and kinetic studies was clearly demonstrated in a comparative study of CO and CO$_2$ hydrogenation on Ru/zeolite and Ru/Al$_2$O$_3$ catalysts.[205]Temperature screening and kinetic measurements revealed that the Ru activity in Ru/zeolite was about 10 times higher compared to the activity in Ru/Al$_2$O$_3$ catalyst. The main reaction intermediate in the predominant reaction route for CO methanation on the Ru/Al$_2$O$_3$ catalyst has been unequivocally identified as HCO$_{ad}$. Nevertheless, HCO$_{ad}$ intermediates have not been identified on the Ru/zeolite catalyst. In this case, the reaction pathway consists of two steps: first CO$_{ad}$ is dissociated and subsequently converted into methane. In addition, surface formates act as spectator species.[205]

Similarly, Schweicher and co-workers employed combined DRIFTS and SSITKA to point out that formate/methylene species observed by DRIFTS are mere spectator intermediates in the ambient pressure Fischer–Tropsch reaction CO on Co/MgO catalysts in a single fixed-bed reactor at 523 K and a H$_2$/CO ratio of 3.[204] The SSITKA experiments showed that the exchange rate of ethane, which is one of the main products of CO hydrogenation, is substantially higher than that of formate/methylene. Moreover, methylene is probably bounded to the surface as CH$_2$ skeleton in either hydrocarbon or carboxylate species, while formate intermediates are adsorbed as bidentate μ_2-species to MgO or Co/MgO interface.

As mentioned previously, the coupling of SSITKA, DRIFTS, and MS techniques helped in the elucidation of the main reaction intermediates and spectator species of some catalytic oxidation reactions[207–212] and the WGS reaction in its forward

or reverse directions.[173,199,203,213−217,219−232] There has been a lot of controversy about the nature of the main intermediates in WGS, which basically are formate (−COOH) or carbonate (−COOOH) species. Meunier and co-workers carried out SSITKA switches between $^{12}CO/^{13}CO$ and in situ DRIFTS analysis to figure out that the reactivity of surface formates over a 2 wt % Pt/CeO_2 catalyst can be increased by a small increase in the reaction temperature during the water−gas shift reaction.[216] The conclusions set the different role of formate species at different temperatures. Although it has been found that formate intermediates are spectators at 433 K, they are the main reaction intermediates at 493 K. This behavior has been related to an increase in the presence of reduced ceria compounds at higher temperatures than 473 K. These results show the importance of the interaction between the formates and the catalytic surface. Efstathiou and co-workers developed an innovative transient experiment to measure the reaction rates of the interaction of formate and CO species by water, which concluded that formate species are not participating in the main reaction network.[173] Similar results have been obtained with catalysts containing TiO_2,[229−231] Al_2O_3[222,223] or other CeO_2-based catalyst containing ZrO_2,[221] doping promoters[219] (i.e., La) as supports or using different metals, such as Au,[219,220] Pd,[222] Rh,[222] CuO.[232] SSITKA-DRIFTS experiments have been carried out to study the presence and evolution of formate and carbonate species over different catalysts under WGS reaction conditions, and it was found that both intermediates are spectators under these conditions. The quantification of the concentration of surface species became crucial to unambiguously demonstrate that the formates seen by DRIFT are spectators for a range of catalysts based on reducible oxides, despite the fact that these species exchanged as fast as CO_2 during SSITKA analysis at higher temperatures.[194]

The composition of the catalytic active site and the essential mechanistic features of the selective catalytic reduction of NO in oxidative atmosphere have also been studied by spectrokinetic techniques.[233−239] The typical isotopic switch that is carried out in this reaction is $^{14}NO/H_2/O_2$ to $^{15}NO/H_2/O_2$ at 1 bar, temperatures between 393 and 573 K, and a wide range of catalyst composition, mainly noble metals coated on inorganic oxides, as seen in Table 4. Despite the differences in catalyst composition, similar results have been obtained when coupling SSITKA to DRIFTS technique. The main intermediates in the process are NO_x species (NO_2^-). The combination of SSITKA and DRIFTS demonstrated the appearance of two active NO_x intermediate species in the reaction network toward N_2 and N_2O formation.[236] Moreover, inactive NO_x intermediate species have been detected. The difference between the NO_x intermediates remains on their structure due to different adsorption over the catalyst. Costa and co-workers found two different NO_x species irreversibly bounded to the support of the catalyst Pt/La−Ce−Mn−O.[233] Haneda and co-workers studied NO decomposition over Co_3O_4 doped with different alkali metals and concluded that NO is decomposed in the interface between the alkali metal and Co_3O_4.[234,235] The results obtained by IR indicated this reaction mechanism: first, NO_2^- molecules are formed from the adsorption of NO onto alkali metals, which are reduced afterward by reacting with other adsorbed NO molecules to generate N_2 over the interface between the alkali metal and the cobalt oxide. The studies carried out in the selective reduction of NO suggest that a mixed nature of the support, which creates

different sites of interaction with the noble metal, is the initiation step to the formation of different NO_x intermediate species who lead to N_2 and N_2O, the main products of this reaction.[233−235,237−240] Additionally, Anastasiadou and co-workers studied the reaction over Ca/La_2O_3 catalyst, and their results demonstrated that the formation of oxygen vacant sites during the reaction promoted the formation of more active chemisorbed NO_x species that contributed to the enhancement of the reaction rate.[236]

Yang and co-workers studied the reverse water−gas shift and methanol synthesis process by measuring simultaneously the site coverage and residence time of adsorbed formates over Cu/SiO_2 catalysts by MS and IR. A wide extent of pressures at temperatures between 413 and 433 K were tested using mixtures of CO_2 and D_2.[203] The residence time of the produced intermediate (DCOO) under steady-state catalytic conditions was measured by $^{12}C/^{13}C$ isotopic transient analysis. The rate of the formate removal reaction, where formate species are converted into a mixture of $CO_2 + 1/2H_2$, was found to be 2 orders of magnitude higher than the catalytic rates for both reverse water−gas shift and methanol synthesis, indicating that these reactions have no influence in the formate surface coverage, and thus, it must be determined by an alternative way. An alternative procedure to measure the formate site coverage is studying the equilibrium between the gas phase ($CO_2 + H_2$) and the production/decomposition of formate species. It has been found that formate is the main intermediate in methanol synthesis and its decomposition rate is faster when both D_2 and CO_2 are present in the feed. Besides, readsorption of methanol on the catalyst was detected and was partially responsible for the additional delay on the residence time of methanol intermediates.

The combined SSITKA and FTIR has also been applied to study the $CO_2−CH_4$ reaction on Rh/Al_2O_3[197,241] and doped ceria-zirconia supported metal catalysts.[242] SSITKA switches between $^{12}CO/^{13}CO$ at 773 K and 1 bar showed that linear CO are active surface species, because the formation of $^{13}CO_2$ is similar to the formation of linear ^{13}CO. Additionally, it was found by in situ IR that hydrogen activates the adsorbed CO_2 to produce linear CO, which were the major species on Rh/Al_2O_3 during the reaction.[197] Linear CO is preferably adsorbed on Rh^0 sites suggesting that metallic Rh crystallites on Al_2O_3 are not oxidized under reaction conditions. The results also indicated that that active carbon-containing species were the main intermediates instead of active oxygen-containing species leading to CO formation.[241]

Specificity of CH_4 dry reforming mechanism for metal-supported doped ceria-zirconia catalysts with high oxygen mobility was elucidated by Bobin and co-workers using a combination of transient kinetic methods (TAP, SSITKA) with pulse microcalorimetry and in situ FTIR spectroscopy.[242] Steady-state reaction of CH_4 dry reforming is described by a simple redox scheme with independent stages of CH_4 and CO_2 activation. This is provided by easy CO_2 dissociation on reduced sites of oxide supports followed by a fast oxygen transfer along the surface/domain boundaries to metal sites where CH_4 is transformed to CO and H_2. The rate-limiting stage is irreversible transformation of CH_4 on metal sites, while CO_2 transformation proceeds much faster being reversible for steady-state surface. Ni + Ru clusters may participate in CO_2 activation and C−O bond breaking in the transition state, making CO_2 capable to reoxidize methane molecules. Strongly bound carbonates are detected as mere spectators.

Theologides and co-workers demonstrated that coupling ex situ DRIFTS and SSITKA experiments is a useful technique in catalytic hydrogenation of nitrates over Pd−Cu-based catalysts.[243] The results pointed out that both the presence of TiO_2 in the support and the presence of oxygen in the feed stream enhance the formation and adsorption of different active N-intermediates on the support or on the surface of Pd−Cu catalysts. In addition, it has been found that Cu clusters increase the reduction rate of nitrates. The combination of SSITKA and DRIFTS techniques allowed detecting a hydrogen spillover process from the Pd−Cu phase to the support.

Balakos and co-workers have studied the ethylene hydroformylation reaction by SSITKA and in situ IR spectroscopy using the SiO_2-based catalyst containing Ce−Rh,[195] Rh[196,244] or Mn−Rh[245,246] as active phase. The kinetic study of Ce−Rh/SiO_2 has been carried out by changing the concentration of the reactant feed from $Ar/^{12}CO/H_2/C_2H_4$ (0.02:1:5:5) to $^{13}CO/H_2/C_2H_4$ (1:5:5) at 453 K and 1 bar.[195] Surface carbonate species were found to be spectator species.

In addition to the powerful ability of combined SSITKA and IR in mechanistic studies, the combined techniques have been approved to enhance the reliability of kinetic modeling. The effect of partial pressures of the reactants in the formation rates of ethane and propionaldehyde and the site coverage of adsorbed CO and acyl species have been evaluated at steady-state on a 4 wt % Rh/SiO_2 catalyst.[244] The dynamic response of $C_2H_5^{13}CHO$ to a ^{13}CO pulse input was used to calculate the site coverage of the intermediates during ethylene hydroformylation. Besides, the coverage of adsorbed CO was measured by in situ IR spectroscopy. In order to elucidate the reaction network, the rate-determining steps and the kinetic parameters for propionaldehyde and ethane formation were compared to a proposed reaction mechanism. The rate expressions for C_2H_5CHO and C_2H_6 formation and the isotherm equations for adsorbed C_2H_5CO and adsorbed CO were derived using the Langmuir−Hinshelwood−Hougen−Watson (LHHW) approach. In the proposed mechanism, it was determined that the hydrogenation of adsorbed C_2H_5CO and the hydrogenation of adsorbed C_2H_5 as rate-determining steps for propionaldehyde and ethane formation, respectively. The combination of the LHHW approach and the proposed mechanism describes successfully the reaction network and the kinetic parameters for both ethane and propionaldehyde formation. It has been observed that both reactions are launched by the insertion of adsorbed linear CO into adsorbed *C_2H_5, species coming from ethylene hydrogenation.[196] This work indicates that the reaction sequence involving CO insertion and subsequent hydrogenation leading to C_{2+} oxygenates is much faster than CO dissociation followed by hydrogenation resulting in hydrocarbons.

Despite that the LHHW kinetic model describes adequately the kinetic data and the reaction pathway, the adsorbed isotherm equation is not able to describe the site coverage dependency of acyl intermediates on CO and H_2 partial pressures due to lack of only one RDS on Mn−Rh/SiO_2 for $CO/H_2/C_2H_4$ reaction.[245] The pseudosteady-state approximation (PSSA) approach, without assumption of a sole rate-determining step, is a valuable tool to solve this concern. The result is the creation of an isotherm equation which describes the kinetic data and adsorbate site coverage accurately. The kinetic of propionaldehyde formation is dependent on both CO insertion into ethyl species and hydrogenation of acyl species.

The combined techniques have also been applied to evaluate the composition of the active sites (Brønsted and Lewis sites) in acid-catalyzed reactions.[247] Hammache and co-workers have tested sulfated zirconia (SZ) catalysts under n-butane isomerization using SSITKA and DRIFTS techniques under different conditions (i.e., in the presence of CO and/or butane or evaluating the effect of temperature in catalyst pretreatment). The results indicated that there is no correlation between the deactivation, due to the formation of carbon layers over the catalyst or the modification of the olefinic sites with the presence of Lewis acid sites. A catalyst pretreatment of SZ catalyst at 773 K caused an enhancement in activity due to an increase in the Brønsted/Lewis ratio and an increase in the concentration of surface intermediates, N_{iso-C4}. These results were not observed when the catalyst was pretreated at 473 or 588 K.

To summarize, the addition of spectroscopic measurements to the SSITKA analysis is a very helpful tool in the elucidation of reaction mechanisms, the improvement of kinetic modeling as well as in the identification of the nature of main intermediates, which may not be detected by using only isotopic transient measurements. The contribution of spectroscopy is also very important in the development of new catalysts due to the fact that the measurement is taken on the catalyst surface allowing the measurement of the interactions between the reaction flow and the active sites under reaction conditions.

6. CONCLUSIONS AND PERSPECTIVES

Steady-State Isotopic Transient Kinetic Analysis (SSITKA) is a powerful technique to determine the number and nature of surface intermediates and the kinetic parameters of catalytic processes. This technique is very well-known since the late 1970s and it helped to study the reaction mechanism of many different and important chemical reactions for the industry. However, on the one hand, it is necessary to use the combination of advanced mathematical modeling to fully understand the reaction mechanism of complex processes where readsorption reactions may take place. On the other hand, it is necessary to involve the combination to other techniques to determine the identity and nature of the intermediates. In this sense, SSITKA has been coupled to spectroscopic techniques to elucidate within real intermediates or spectators in the reaction mechanism. Besides, a lot of information about the reaction pathway can be obtained when SSITKA is combined to other methods, such as kinetic modeling. This will be the guideline for the near future, the combination of the advantages of SSITKA with the advantages of other techniques to obtain as much information as possible under reaction conditions to clarify the pathways of chemical reactions with complicated reaction mechanisms.

■ AUTHOR INFORMATION

Corresponding Authors
*E-mail: de.chen@ntnu.no.
*E-mail: anders.holmen@ntnu.no.

Notes
The authors declare no competing financial interest.

■ ACKNOWLEDGMENTS

■ REFERENCES

(1) Chorkendorff, I.; Niemantsverdriet, J. W. In *Conceptsof Modern Catalysis and Kinetics*; Wiley-VCH Verlag: Weinheim, 2007; pp 1−22.

(2) Kang, H. C.; Weinberg, W. H. *Chem. Rev.* **1995**, *95*, 667−676.

(3) Berger, R. J.; Kapteijn, F.; Moulijn, J. A.; Marin, G. B.; De Wilde, J.; Olea, M.; Chen, D.; Holmen, A.; Lietti, L.; Tronconi, E.; Schuurman, Y. *Appl. Catal., A* **2008**, *342*, 3−28.

(4) Shannon, S. L.; Goodwin, J. G. *Chem. Rev.* **1995**, *95*, 677−695.

(5) Biloen, P. *J. Mol. Catal.* **1983**, *21*, 17−24.

(6) Happel, J. *Chem. Eng. Sci.* **1978**, *33*, 1567−1569.

(7) Olaru, I.; Almasan, V.; Samoila, C.; Ursutiu, D.; Cotfas, P.; Cotfas, D. *Metal. Int.* **2011**, *16*, 49−52.

(8) Biloen, P.; Helle, J. N.; Van den Berg, F. G. A.; Sachtler, W. M. H. *J. Catal.* **1983**, *81*, 450−463.

(9) Mirodatos, C. *Catal. Today* **1991**, *9*, 83−95.

(10) Goodwin, J. G.; Soo, K.; Rhodes, W. D. In *Catalysis*; Spivey, J. J.; Roberts, G. W., Eds.; Catalysis; Royal Society of Chemistry: Cambridge, 2004; Vol. *17*, pp 320−347.

(11) Pansare, S. S.; Sirijaruphan, A.; Goodwin, J. G. *J. Catal.* **2005**, *234*, 151−160.

(12) Mirodatos, C. *Stud. Surf. Sci. Catal.* **1998**, *119*, 99−106.

(13) Kondratenko, E. V. *Catal. Today* **2010**, *157*, 16−23.

(14) McClaine, B.; Davis, R. J. *J. Catal.* **2002**, *211*, 379−386.

(15) McClaine, B.; Davis, R. J. *J. Catal.* **2002**, *210*, 387−396.

(16) Nwalor, J. U.; Goodwin, J. G. *Top. Catal.* **1994**, *1*, 285−293.

(17) Siporin, S. E. *J. Catal.* **2004**, *222*, 315−322.

(18) Brundage, M. A.; Chuang, S. S. C. *J. Catal.* **1996**, *164*, 94−108.

(19) Kondratenko, E. V.; Ovsitser, O.; Radnik, J.; Schneider, M.; Kraehnert, R.; Dingerdissen, U. *Appl. Catal., A* **2007**, *319*, 98−110.

(20) Liu, C.; Ozkan, U. S. *J. Phys. Chem. A* **2005**, *109*, 1260−1268.

(21) Ovsitser, O.; Kondratenko, E. V. *Catal. Today* **2009**, *142*, 138−142.

(22) Kim, S. Y.; Goodwin, J. G.; Galloway, D. *Catal. Lett.* **2000**, *64*, 1−8.

(23) Kim, S. Y.; Goodwin, J. G.; Galloway, D. *Catal. Today* **2000**, *63*, 21−32.

(24) Kim, S. Y.; Goodwin, J. G.; Hammache, S.; Auroux, A.; Galloway, D. *J. Catal.* **2001**, *201*, 1−12.

(25) Kim, S. Y.; Lohitharn, N.; Goodwin, J. G.; Olindo, R.; Pinna, F.; Canton, P. *Catal. Commun.* **2006**, *7*, 209−213.

(26) Kao, J. Y.; Piet-Lahanier, H.; Walter, E.; Happel, J. *J. Catal.* **1992**, *133*, 383−396.

(27) VanDijk, H. A. J.; Hoebink, J. H. B. J.; Schouten, J. C. *Top. Catal.* **2003**, *26*, 111−119.

(28) Bertole, C.; Mims, C. A.; Kiss, G. *J. Catal.* **2004**, *221*, 191−203.

(29) Agnelli, M.; Swaan, H. M.; Marquez-Alvarez, C.; Martin, G. A.; Mirodatos, C. *J. Catal.* **1998**, *175*, 117−128.

(30) Pansare, S.; Sirijaruphan, A.; Goodwin, J. G. In *Isotopes in Heterogeneous Catalysis*; Hutchings, G. J., Ed.; World Scientific Publishing Co.: London, 2006; Catalytic Science Series, Vol. *4*, pp 183−206.

(31) Ali, S. H.; Goodwin, J. G. *J. Catal.* **1997**, *171*, 339−344.

(32) Basallote, M. G.; Bernal, S.; Gatica, J. M.; Pozo, M. *Appl. Catal., A* **2002**, *232*, 39−50.

(33) Hedrick, S. A.; Chuang, S. S. C.; Brundage, M. A. *J. Catal.* **1999**, *185*, 73−90.

(34) Peil, K. P.; Marcelin, G.; Goodwin, J. G. In *Methane Conversion by Oxidative Processes*; Wolf, E. E., Ed.; Springer Netherlands: New York, 1992; pp 139−145.

(35) Drochner, A.; Kampe, P.; Kunert, J.; Ott, J.; Vogel, H. *Appl. Catal., A* **2005**, *289*, 74−83.

(36) Kampe, P.; Giebeler, L.; Samuelis, D.; Kunert, J.; Drochner, A.; Haass, F.; Adams, A. H.; Ott, J.; Endres, S.; Schimanke, G.; Buhrmester, T.; Martin, M.; Fuess, H.; Vogel, H. *Phys. Chem. Chem. Phys.* **2007**, *9*, 3577−3589.

(37) Endres, S.; Kampe, P.; Kunert, J.; Drochner, A.; Vogel, H. *Appl. Catal., A* **2007**, *325*, 237−243.

(38) Drochner, A.; Kampe, P.; Blickhan, N.; Jekewitz, T.; Vogel, H. *Chemie Ing. Technol.* **2011**, *83*, 1667−1680.

(39) Krauß, K.; Drochner, A.; Fehlings, M.; Kunert, J.; Vogel, H. *J. Mol. Catal. A: Chem.* **2002**, *177*, 237−245.

(40) Kuhn, J. N.; Matter, P. H.; Millet, J. M. M.; Watson, R. B.; Ozkan, U. S. *J. Phys. Chem. C* **2008**, *112*, 12468−12476.

(41) Peil, K. P.; Goodwin, J. G.; Marcelin, G. *J. Catal.* **1991**, *131*, 143−155.

(42) Peil, K. P.; Marcelin, G.; Goodwin, J. G.; Kiennemann, A. In *Novel Production Methods for Ethylene, Light Hydrocarbons and Aromatics*; Albright, L. F., Ed.; Marcel Dekker Inc.: New York, 1992; pp 61−74.

(43) Hoost, T.; Goodwin, J. G. *J. Catal.* **1992**, *134*, 678−690.

(44) Shannon, S. L.; Goodwin, J. G. *Appl. Catal., A* **1997**, *151*, 3−26.

(45) Govender, N. S.; Botes, F. G.; de Croon, M. H. J. M.; Schouten, J. C. *J. Catal.* **2014**, *312*, 98−107.

(46) VanDijk, H. A. J.; Hoebink, J. H. B. J.; Schouten, J. C. *Top. Catal.* **2003**, *26*, 163−171.

(47) Yang, J.; Qi, Y.; Zhu, J.; Zhu, Y.; Chen, D.; Holmen, A. *J. Catal.* **2013**, *308*, 37−49.

(48) VanDijk, H. A. J.; Hoebink, J. H. B. J.; Schouten, J. C. *Chem. Eng. Sci.* **2001**, *56*, 1211−1219.

(49) Öcal, M.; Oukaci, R.; Marcelin, G.; Agarwal, S. K. *Ind. Eng. Chem. Res.* **1994**, *33*, 2930−2934.

(50) Burch, R.; Shestov, A. A.; Sullivan, J. A. *J. Catal.* **1999**, *188*, 69−82.

(51) Burch, R.; Shestov, A. A.; Sullivan, J. A. *J. Catal.* **1999**, *182*, 497−506.

(52) Burch, R. *Top. Catal.* **2003**, *24*, 97−102.

(53) Burch, R.; Shestov, A. A.; Sullivan, J. A. *J. Catal.* **1999**, *186*, 353−361.

(54) Sadovskaya, E.; Suknev, A. P.; Pinaeva, L. G.; Goncharov, V. B.; Mirodatos, C.; Balzhinimaev, B. S. *Stud. Surf. Sci. Catal.* **2000**, *103 B*, 1505−1510.

(55) Sadovskaya, E.; Suknev, A. P.; Pinaeva, L. G.; Goncharov, V. B.; Balzhinimaev, B. S.; Chupin, C.; Mirodatos, C. *J. Catal.* **2001**, *201*, 159−168.

(56) Sadovskaya, E.; Suknev, A. P.; Pinaeva, L. G.; Goncharov, V. B.; Balzhinimaev, B. S.; Chupin, C.; Pérez-Ramírez, J.; Mirodatos, C. *J. Catal.* **2004**, *225*, 179−189.

(57) Sadovskaya, E.; Suknev, A. P.; Goncharov, V. B.; Balzhinimaev, B. S.; Mirodatos, C. *Kinet. Catal* **2004**, *45*, 436−445.

(58) Schuurman, Y.; Van Veen, A. C.; Chupin, C.; Mirodatos, C.; Veen, A. C. *Top. Catal* **2006**, *39*, 45−52.

(59) Burch, R.; Coleman, M. D. *J. Catal.* **2002**, *208*, 435−447.

(60) Sullivan, J. A.; Burch, R.; Shestov, A. A. *Chem. Eng. Res. Des.* **2000**, *78*, 947−953.

(61) Avgouropoulos, G. *Catal. Commun.* **2009**, *10*, 682−686.

(62) Papavasiliou, J.; Avgouropoulos, G.; Ioannides, T. *Appl. Catal., B* **2009**, *88*, 490−496.

(63) Polychronopoulou, K.; Costa, C. N.; Efstathiou, A. M. *Catal. Today* **2006**, *112*, 89−93.

(64) Polychronopoulou, K.; Efstathiou, A. M. *Catal. Today* **2006**, *116*, 341−347.

(65) Nijhuis, T. A.; Sacaliuc-Parvulescu, E.; Govender, N. S.; Schouten, J. C.; Weckhuysen, B. M. *J. Catal.* **2009**, *265*, 161−169.

(66) Oukaci, R.; Gallaher, G.; Goodwin, J. G.; Blackmond, D. G. *Abstr. Pap. Am. Chem. Soc.* **1991**, *202*, 187−188.

(67) Oukaci, R.; Blackmond, D. G.; Goodwin, J. G.; Gallaher, G.; *Catalytic Control of Air Pollution*; American Chemical Society: Washington, DC, 1992; Vol. *495*, pp 61−7210.1021/bk-1992-0495.ch005.

(68) Granger, P.; Pietrzyk, S. *Comptes Rendus Chim* **2014**, *17*, 656−671.

(69) Efstathiou, A. M.; Verykios, X. *Appl. Catal. A Gen* **1997**, *151*, 109−166.

(70) Öcal, M.; Oukaci, R.; Marcelin, G.; Jang, B. W. L.; Spivey, J. J. *Catal. Today* **2000**, *59*, 205−217.

(71) Sadykov, V. A.; Kuznetsova, T. G.; Frolova-Borchert, Y. V.; Alikina, G. M.; Lukashevich, A. I.; Rogov, V. A.; Muzykantov, V. S.; Pinaeva, L. G.; Sadovskaya, E.; Ivanova, Y. A.; Paukshtis, E. A.;

Mezentseva, N. V.; Batuev, L. C.; Parmon, V. N.; Neophytides, S.; Kemnitz, E.; Scheurell, K.; Mirodatos, C.; Van Veen, A. C. *Catal. Today* **2006**, *117*, 475−483.

(72) Machocki, A.; Rotko, M.; Gac, W. *Top. Catal* **2009**, *52*, 1085−1097.

(73) Machocki, A.; Rotko, M.; Stasinska, B. *Catal. Today* **2008**, *137*, 312−317.

(74) Rotko, M.; Machocki, A.; Stasinska, B. *Appl. Surf. Sci.* **2010**, *256*, 5585−5589.

(75) Calla, J. T.; Davis, R. J. *J. Phys. Chem. B* **2005**, *109*, 2307−2314.

(76) Calla, J. T.; Davis, R. J. *J. Catal.* **2006**, *241*, 407−416.

(77) Calla, J. T.; Bore, M. T.; Datye, A. K.; Davis, R. J. *J. Catal.* **2006**, *238*, 458−467.

(78) Frank, B.; Rinaldi, A.; Blume, R.; Schlögl, R.; Su, D. S. *Chem. Mater.* **2010**, *22*, 4462−4470.

(79) Ouyang, X.; Scott, S. L. *Mater. Res. Soc. Symp. Proc.* **2010**, *Vol.1217*, 21−26.

(80) Zhang, R.; Haddadin, T.; Rubiano, D. P.; Nair, H.; Polster, C. S.; Baertsch, C. D. *ACS Catal.* **2011**, *1*, 519−525.

(81) Heracleous, E.; Lemonidou, A. A. *J. Catal.* **2006**, *237*, 175−189.

(82) Glazneva, T. S.; Kotsarenko, N. S.; Paukshtis, E. A. *Kinet. Catal.* **2008**, *49*, 859−867.

(83) Bajusz, I. G.; Goodwin, J. G. *Langmuir* **1997**, *13*, 6550−6554.

(84) Bajusz, I. G.; Goodwin, J. G.; Galloway, D.; Greenlay, N. *Langmuir* **1998**, *14*, 2876−2883.

(85) Siporin, S. E.; McClaine, B. C.; Davis, R. J. *Langmuir* **2003**, *19*, 4707−4713.

(86) Yang, J.; Ma, W.; Chen, D.; Holmen, A.; Davis, B. H. *Appl. Catal., A* **2014**, *470*, 250−260.

(87) Krylova, A. Y. *Solid Fuel Chem.* **2014**, *48*, 22−35.

(88) Patzlaff, J.; Liu, Y.; Graffmann, C.; Gaube, J. *Appl. Catal., A* **1999**, *186*, 109−119.

(89) Todic, B.; Ma, W.; Jacobs, G.; Davis, B. H.; Bukur, D. B. *J. Catal.* **2014**, *311*, 325−338.

(90) Weststrate, C. J.; Ciobîcă, I. M.; Saib, A. M.; Moodley, D. J.; Niemantsverdriet, J. W. *Catal. Today* **2014**, *228*, 106−112.

(91) Lögdberg, S.; Tristantini, D.; Borg, Ø.; Ilver, L.; Gevert, B.; Järås, S.; Blekkan, E. A.; Holmen, A. *Appl. Catal., B* **2009**, *89*, 167−182.

(92) Baliban, R. C.; Elia, J. A.; Weekman, V.; Floudas, C. A. *Comput. Chem. Eng.* **2012**, *47*, 29−56.

(93) Zhang, Q.; Deng, W.; Wang, Y. *J. Energy Chem.* **2013**, *22*, 27−38.

(94) Todic, B.; Ma, W.; Jacobs, G.; Davis, B. H.; Bukur, D. B. *Catal. Today* **2014**, *228*, 32−39.

(95) Yang, J.; Chen, D.; Holmen, A. *Catal. Today* **2012**, *186*, 99−108.

(96) Schanke, D.; Vada, S.; Blekkan, E. A.; Hilmen, A. M.; Hoff, A.; Holmen, A. *J. Catal.* **1995**, *156*, 85−95.

(97) Vada, S.; Hoff, A.; Ådnanes, E.; Schanke, D.; Holmen, A. *Top. Catal* **1995**, *2*, 155−162.

(98) Kogelbauer, A.; Goodwin, J. G.; Oukaci, R. *J. Catal.* **1996**, *160*, 125−133.

(99) Panpranot, J.; Goodwin, J. G.; Sayari, A. *J. Catal.* **2002**, *211*, 530−539.

(100) Bertole, C.; Kiss, G.; Mims, C. A. *J. Catal.* **2004**, *223*, 309−318.

(101) Haddad, G.; Chen, B.; Goodwin, J. G. *J. Catal.* **1996**, *161*, 274−281.

(102) Vada, S.; Chen, B.; Goodwin, J. G. *J. Catal.* **1995**, *153*, 224−231.

(103) Vada, S.; Kazi, A. M.; Bedu-Addo, F. K.; Chen, B.; Goodwin, J. G. *Stud. Surf. Sci. Catal.* **1994**, *81*, 443−448.

(104) Den Breejen, J. P.; Frey, A. M.; Yang, J.; Holmen, A.; Schooneveld, M. M.; Groot, F. M. F.; Stephan, O.; Bitter, J. H.; Jong, K. P. *Top. Catal* **2011**, *54*, 768−777.

(105) Borg, Ø.; Hammer, N.; Enger, B. C.; Myrstad, R.; Lindvåg, O. A.; Eri, S.; Skagseth, T. H.; Rytter, E. *J. Catal.* **2011**, *279*, 163−173.

(106) Patanou, E.; Lillebø, A. H.; Yang, J.; Chen, D.; Holmen, A.; Blekkan, E. A. *Ind. Eng. Chem. Res.* **2013**, *53*, 1787−1793.

(107) Lillebø, A. H.; Patanou, E.; Yang, J.; Blekkan, E. A.; Holmen, A. *Catal. Today* **2013**, *215*, 60−66.

(108) Balonek, C. M.; Lillebø, A. H.; Rane, S.; Rytter, E.; Schmidt, L. D.; Holmen, A. *Catal. Lett.* **2010**, *138*, 8−13.

(109) Lohitharn, N.; Goodwin, J. G.; Lotero, E. *J. Catal.* **2008**, *260*, 7−16.

(110) Graf, B.; Schulte, H.; Muhler, M. *J. Catal.* **2010**, *276*, 66−75.

(111) Lohitharn, N.; Goodwin, J. G.; Lotero, E. *J. Catal.* **2008**, *255*, 104−113.

(112) Lohitharn, N.; Goodwin, J. G.; Lotero, E. *J. Catal.* **2008**, *257*, 142−151.

(113) Lohitharn, N.; Goodwin, J. G. *Catal. Commun.* **2009**, *10*, 758−762.

(114) Al-Sayari, S. *Ceram. Int.* **2014**, *40*, 723−728.

(115) Govender, N. S.; de Croon, M. H. J. M.; Schouten, J. C. *Appl. Catal., A* **2010**, *373*, 81−89.

(116) Hoost, T.; Goodwin, J. G. *J. Catal.* **1992**, *137*, 22−35.

(117) Bajusz, I. G.; Kwik, D. J.; Goodwin, J. G. *Catal. Lett.* **1997**, *48*, 151−157.

(118) Vada, S.; Goodwin, J. G. *J. Phys. Chem.* **1995**, *99*, 9479−9484.

(119) Ali, S. H.; Goodwin, J. G. *J. Catal.* **1998**, *176*, 3−13.

(120) Rohr, F.; Holmen, A.; Barbo, K. K.; Warloe, P.; Blekkan, E. A. *Stud. Surf. Sci. Catal.* **1998**, *119*, 107−112.

(121) Rohr, F.; Lindvåg, O. A.; Holmen, A.; Blekkan, E. A. *Catal. Today* **2000**, *58*, 247−254.

(122) Jongsomjit, B.; Panpranot, J.; Goodwin, J. G. *J. Catal.* **2003**, *215*, 66−77.

(123) Enger, B. C.; Frøseth, V.; Yang, J.; Rytter, E.; Holmen, A. *J. Catal.* **2013**, *297*, 187−192.

(124) Enger, B. C.; Fossan, Å. L.; Borg, Ø.; Rytter, E.; Holmen, A. *J. Catal.* **2011**, *284*, 9−22.

(125) Mo, X.; Tsai, Y. T.; Gao, J.; Mao, D.; Goodwin, J. G. *J. Catal.* **2012**, *285*, 208−215.

(126) Tsai, Y. T.; Mo, X.; Goodwin, J. G. *Top. Catal.* **2012**, *55*, 757−770.

(127) Rane, S.; Borg, Ø.; Yang, J.; Rytter, E.; Holmen, A. *Appl. Catal., A* **2010**, *388*, 160−167.

(128) Phan, X.; Yang, J.; Bakhtiary-Davijnay, H.; Myrstad, R.; Venvik, H.; Holmen, A. *Catal. Lett.* **2011**, *141*, 1739−1745.

(129) Gonzalez-Carballo, J. M.; Yang, J.; Holmen, A.; García-Rodríguez, S.; Rojas, S.; Ojeda, M.; Fierro, J. L. G. *J. Catal.* **2011**, *284*, 102−108.

(130) Yang, J.; Tveten, E. Z.; Chen, D.; Holmen, A. *Langmuir* **2010**, *26*, 16558−16567.

(131) Den Breejen, J. P.; Radstake, P. B.; Bezemer, G. L.; Bitter, J. H.; Frøseth, V.; Holmen, A.; Jong, K. P. *J. Am. Chem. Soc.* **2009**, *131*, 7197−7203.

(132) Cant, N. W.; Bell, A. T. *J. Catal.* **1982**, *73*, 257−271.

(133) Iglesia, E.; Soled, S. L.; Fiato, R. A. *J. Catal.* **1992**, *137*, 212−224.

(134) Bezemer, G. L.; Bitter, J. H.; Kuipers, H. P. C. E.; Oosterbeek, H.; Holewijn, J. E.; Xu, X.; Kapteijn, F.; van Dillen, A. J.; de Jong, K. P. *J. Am. Chem. Soc.* **2006**, *128*, 3956−3964.

(135) Tsai, Y. T.; Goodwin, J. G. *J. Catal.* **2011**, *281*, 128−136.

(136) Khodakov, A. Y. *Catal. Today* **2009**, *144*, 251−257.

(137) Frøseth, V.; Holmen, A. *Top. Catal.* **2007**, *45*, 45−50.

(138) Bajusz, I. G.; Goodwin, J. G. *J. Catal.* **1997**, *169*, 157−165.

(139) Panpranot, J.; Goodwin, J. G.; Sayari, A. *J. Catal.* **2003**, *213*, 78−85.

(140) Rothaemel, M.; Hanssen, K. F.; Blekkan, E. A.; Schanke, D.; Holmen, A. *Catal. Today* **1997**, *38*, 79−84.

(141) Hanssen, K. F.; Blekkan, E. A.; Schanke, D.; Holmen, A.; Froment, G. F.; Waugh, K. C. *Stud. Surf. Sci. Catal.* **1997**, *109*, 193−202.

(142) Bertole, C.; Mims, C. A.; Kiss, G. *J. Catal.* **2002**, *210*, 84−96.

(143) Frøseth, V.; Storsæter, S.; Borg, Ø.; Blekkan, E. A.; Rønning, M.; Holmen, A. *Appl. Catal., A* **2005**, *289*, 10−15.

(144) Borg, Ø.; Storsæter, S.; Eri, S.; Wigum, H.; Rytter, E.; Holmen, A. *Catal. Lett.* **2006**, *107*, 95−102.

(145) Storsæter, S.; Borg, Ø.; Blekkan, E. a. A.; Tøtdal, B.; Holmen, A. *Catal. Today* **2005**, *100*, 343−347.

(146) Storsæter, S.; Borg, Ø.; Blekkan, E. A.; Holmen, A. *J. Catal.* **2005**, *231*, 405−419.

(147) Jacobs, G.; Das, T. K.; Li, J.; Luo, M.; Patterson, P. M.; Davis, B. H. *Stud. Surf. Sci. Catal.* **2007**, *163*, 217−253.

(148) Dalai, A. K.; Das, T. K.; Chaudhari, K. V.; Jacobs, G.; Davis, B. H. *Appl. Catal., A* **2005**, *289*, 135−142.

(149) Jacobs, G.; Patterson, P. M.; Das, T. K.; Luo, M.; Davis, B. H. *Appl. Catal., A* **2004**, *270*, 65−76.

(150) Krishnamoorthy, S.; Tu, M.; Ojeda, M.; Pinna, D.; Iglesia, E. *J. Catal.* **2002**, *211*, 422−433.

(151) Hilmen, A. M.; Schanke, D.; Hanssen, K. F.; Holmen, A. *Appl. Catal., A* **1999**, *186*, 169−188.

(152) Sudsakorn, K.; Goodwin, J. G.; Adeyiga, A. A. *J. Catal.* **2003**, *213*, 204−210.

(153) Wang, Y.; Chernavskii, P. A.; Khodakov, A. Y. *J. Catal.* **2012**, *286*, 51−61.

(154) Dalai, A. K.; Davis, B. H. *Appl. Catal., A* **2008**, *348*, 1−15.

(155) Davis, B. H. *Catal. Today* **2009**, *141*, 25−33.

(156) Lögdberg, S.; Lualdi, M.; Järås, S.; Walmsley, J. C.; Blekkan, E. A.; Rytter, E.; Holmen, A. *J. Catal.* **2010**, *274*, 84−98.

(157) Teng, B. T.; Chang, J.; Zhang, C. H.; Cao, D. B.; Yang, J.; Liu, Y.; Guo, X. H.; Xiang, H. W.; Li, Y. W. *Appl.Catal., A* **2006**, *301*, 39−50.

(158) Balzhinimaev, B. S.; Sadovskaya, E.; Suknev, A. P. *Chem. Eng. J.* **2009**, *154*, 2−8.

(159) Marquez-Alvarez, C.; Martin, G. A.; Mirodatos, C. *Stud. Surf. Sci.Catal.* **1998**, *119*, 155−160.

(160) Swart, J. W. A.; Krishna, R. *Chem. Eng. Process. Process Intensif.* **2002**, *41*, 35−47.

(161) Gao, J.; Mo, X.; Goodwin, J. G. *J. Catal.* **2010**, *275*, 211−217.

(162) Gao, J.; Mo, X.; Goodwin, J. G. *Catal. Today* **2011**, *160*, 44−49.

(163) Tsai, Y. T.; Mo, X.; Goodwin, J. G. *J. Catal.* **2012**, *285*, 242−250.

(164) Shou, H.; Davis, R. J. *J. Catal.* **2013**, *306*, 91−99.

(165) Van Santen, R. A.; Ghouri, M. M.; Shetty, S.; Hensen, E. M. H. *Catal. Sci. Technol.* **2011**, *1*, 891−911.

(166) Van Santen, R. A.; Markvoort, A. J. *Faraday Discuss.* **2013**, *162*, 267−279.

(167) Storsæter, S.; Chen, D.; Holmen, A. *Surf. Sci.* **2006**, *600*, 2051−2063.

(168) Rothaemel, M.; Hanssen, K. F.; Blekkan, E. A.; Schanke, D.; Holmen, A. *Catal. Today* **1998**, *40*, 171−179.

(169) Otarod, M.; Happel, J.; Soong, Y.; Walter, E.; Pronzato, L. *Appl. Catal., A* **1997**, *151*, 97−107.

(170) Pontes, M.; Yokomizo, G. H.; Bell, A. T. *J. Catal.* **1987**, *104*, 147−155.

(171) Sage, V.; Burke, N. *Catal. Today* **2011**, *178*, 137−141.

(172) Harmsen, J. M. A.; Hoebink, J. H. B. J.; Schouten, J. C. *Chem. Eng. Sci.* **2001**, *56*, 2019−2035.

(173) Kalamaras, C. M.; Americanou, S.; Efstathiou, A. M. *J. Catal.* **2011**, *279*, 287−300.

(174) Kalamaras, C. M.; Gonzalez, I. D.; Navarro, R. M.; Fierro, J. L. G.; Efstathiou, A. M. *J. Phys. Chem. C* **2011**, *115*, 11595−11610.

(175) Mei, D.; Gutowski, M.; Neurock, M.; Yang, Y.; Disselkamp, R. S.; Campbell, C. T. *ACS National Meeting Book of Abstracts*; **2006**; Vol. 232, p 1.

(176) Dave, P. N.; Malpani, P. R.; Pande, S. K. *Recent Progress in Chemistry and Chemical Engineering Research*; Nova Science Publishers, Inc.: Hauppauge NY, 2011; pp 107−172.

(177) Hartfelder, U.; Szlachetko, J.; Sá, J.; Van Bokhoven, J. A. *Analyst* **2012**, *137*, 5374−5381.

(178) Stockwell, D. M.; Bennett, C. O. *J. Catal.* **1988**, *110*, 354−363.

(179) Govender, N. S.; Botes, F. G.; de Croon, M. H. J. M.; Schouten, J. C. *J. Catal.* **2008**, *260*, 254−261.

(180) Sirijaruphan, A.; Goodwin, J. G.; Rice, R. W.; Wei, D.; Butcher, K. R.; Roberts, G. W.; Spivey, J. J. *Appl. Catal., A* **2005**, *281*, 1−9.

(181) Sirijaruphan, A.; Goodwin, J. G.; Rice, R. W.; Wei, D.; Butcher, K. R.; Roberts, G. W.; Spivey, J. J. *Appl. Catal., A* **2005**, *281*, 11−18.

(182) Davies, J. C.; Nielsen, R. M.; Thomsen, L. B.; Chorkendorff, I.; Logadóttir, A.; Lodziana, Z.; Nørskov, J. K.; Li, W. X.; Hammer, B.; Longwitz, S. R.; Schnadt, J.; Vestergaard, E. K.; Vang, R. T.; Besenbacher, F. *Fuel Cells* **2004**, *4*, 309−319.

(183) Davies, J. C.; Bonde, J.; Logadóttir, A.; Nørskov, J. K.; Chorkendorff, I. *Fuel Cells* **2005**, *5*, 429−435.

(184) Davies, J. C.; Tsotridis, G.; Varlam, M.; Valkiers, S.; Berglund, M.; Taylor, P. *Int. J. Mass Spectrom.* **2010**, *291*, 152−158.

(185) Oetjen, H. F.; Schmidt, V. M.; Stimming, U.; Trila, F. *J. Electrochem. Soc.* **1996**, *143*, 3838−3842.

(186) Watanabe, M.; Motoo, S. *J. Electroanal. Chem. Interfacial Electrochem.* **1975**, *60*, 267−273.

(187) Lu, C.; Rice, C.; Masel, R. I.; Babu, P. K.; Waszczuk, P.; Kim, H. S.; Oldfield, E.; Wieckowski, A. *J. Phys. Chem. B* **2002**, *106*, 9581−9589.

(188) Igarashi, H.; Fujino, T.; Zhu, Y.; Uchida, H.; Watanabe, M. *Phys. Chem. Chem. Phys.* **2001**, *3*, 306−314.

(189) El-Roz, M.; Bazin, P.; Daturi, M.; Thibault-Starzyk, F. *ACS Catal.* **2013**, *3*, 2790−2798.

(190) Van Doorslaer, S.; Murphy, D. M. *Top. Curr. Chem.* **2012**, *321*, 1−39.

(191) Dalziel, K.; O'Brien, J. R. *Biochem. J.* **1957**, *67*, 124−136.

(192) Tamaru, K. *Adv. Catal.* **1964**, *15*, 65−90.

(193) Ueno, A.; Onishi, T.; Tamaru, K. *Trans. Faraday Soc.* **1970**, *66*, 756−763.

(194) Meunier, F. C. *Catal. Today* **2010**, *155*, 164−171.

(195) Srinivas, G.; Chuang, S. S. C.; Balakos, M. W. *AlChE J.* **1993**, *39*, 530−532.

(196) Balakos, M. W.; Chuang, S. S. C.; Srinivas, G. *J. Catal.* **1993**, *140*, 281−285.

(197) Stevens, R. W.; Chuang, S. S. C. *J. Phys. Chem. B* **2004**, *108*, 696−703.

(198) Chuang, S. S. C.; Guzman, F. *Top. Catal.* **2009**, *52*, 1448−1458.

(199) Goguet, A.; Meunier, F. C.; Tibiletti, D.; Breen, J. P.; Burch, R. *J. Phys. Chem. B* **2004**, *108*, 20240−20246.

(200) Yang, Y.; Disselkamp, R. S.; Szanyi, J.; Peden, C. H. F.; Campbell, C. T.; Goodwin, J. G. *Rev. Sci. Instrum.* **2006**, *77*, 094104.

(201) Stockwell, D. M.; Chung, J. S.; Bennett, C. O. *J. Catal.* **1988**, *112*, 135−144.

(202) Balakos, M. W.; Chuang, S. S. C.; Srinivas, G.; Brundage, M. A. *J. Catal.* **1995**, *157*, 51−65.

(203) Yang, Y.; Mims, C. A.; Disselkamp, R. S.; Peden, C. H. F.; Campbell, C. T. *Top. Catal.* **2009**, *52*, 1440−1447.

(204) Schweicher, J.; Bundhoo, A.; Frennet, A.; Kruse, N.; Daly, H.; Meunier, F. C. *J. Phys. Chem. C* **2010**, *114*, 2248−2255.

(205) Eckle, S.; Denkwitz, Y.; Behm, R. J. *J. Catal.* **2010**, *269*, 255−268.

(206) Eckle, S.; Anfang, H. G.; Behm, R. J. *J. Phys. Chem. C* **2011**, *115*, 1361−1367.

(207) Matyshak, V. A.; Krylov, O. V. *Catal. Today* **1995**, *25*, 1−87.

(208) Van Neer, F.; Bliek, A. *Chem. Eng. Sci.* **1999**, *54*, 4483−4499.

(209) Cheung, P.; Liu, H.; Iglesia, E. *J. Phys. Chem. B* **2004**, *108*, 18650−18658.

(210) Rajasree, R.; Hoebink, J. H. B. J.; Schouten, J. C. *J. Catal.* **2004**, *223*, 36−43.

(211) Bazin, P.; Thomas, S.; Marie, O.; Daturi, M. *Catal. Today* **2012**, *182*, 3−11.

(212) Engeldinger, J.; Richter, M.; Bentrup, U. *Phys. Chem. Chem. Phys.* **2012**, *14*, 2183−2191.

(213) Meunier, F. C.; Tibiletti, D.; Goguet, A.; Reid, D.; Burch, R. *Appl. Catal., A* **2005**, *289*, 104−112.

(214) Tibiletti, D.; Goguet, A.; Reid, D.; Meunier, F. C.; Burch, R. *Catal.Today* **2006**, *113*, 94−101.

(215) Meunier, F. C.; Tibiletti, D.; Goguet, A.; Burch, R. *Oil Gas Sci. Technol.- Rev. l'IFP* **2006**, *61*, 497−502.

(216) Meunier, F. C.; Tibiletti, D.; Goguet, A.; Shekhtman, S.; Hardacre, C.; Burch, R. *Catal. Today* **2007**, *126*, 143−147.

(217) Meunier, F. C.; Goguet, A.; Hardacre, C.; Burch, R.; Thompsett, D. *J. Catal.* **2007**, *252*, 18−22.

(218) Aranifard, S.; Ammal, S. C.; Heyden, A. *J. Catal.* **2014**, *309*, 314−324.

(219) Meunier, F. C.; Reid, D.; Goguet, A.; Shekhtman, S.; Hardacre, C.; Burch, R.; Deng, W.; Flytzani-Stephanopoulos, M. *J. Catal.* **2007**, *247*, 277−287.

(220) Daly, H.; Ni, J.; Thompsett, D.; Meunier, F. C. *J. Catal.* **2008**, *254*, 238−243.

(221) Tibiletti, D.; Meunier, F. C.; Goguet, A.; Reid, D.; Burch, R.; Boaro, M.; Vicario, M.; Trovarelli, A. *J. Catal.* **2006**, *244*, 183−191.

(222) Olympiou, G. G.; Kalamaras, C. M.; Zeinalipour-Yazdi, C. D.; Efstathiou, A. M. *Catal. Today* **2007**, *127*, 304−318.

(223) Kalamaras, C. M.; Olympiou, G. G.; Efstathiou, A. M. *Catal. Today* **2008**, *138*, 228−234.

(224) Costa, C. N.; Efstathiou, A. M. *J. Phys. Chem. C* **2007**, *111*, 3010−3020.

(225) Kalamaras, C. M.; Dionysiou, D. D.; Efstathiou, A. M. *ACS Catal.* **2012**, *2*, 2729−2742.

(226) Kalamaras, C. M.; Petallidou, K. C.; Efstathiou, A. M. *Appl. Catal., B* **2013**, *136−137*, 225−238.

(227) Petallidou, K. C.; Kalamaras, C. M.; Efstathiou, A. M. *Catal. Today* **2014**, *228*, 183−193.

(228) Jacobs, G.; Davis, B. H. *Appl. Catal., A* **2007**, *333*, 192−201.

(229) Kalamaras, C. M.; Panagiotopoulou, P.; Kondarides, D. I.; Efstathiou, A. M. *J. Catal.* **2009**, *264*, 117−129.

(230) Wang, J.; Kispersky, V. F.; Nicholas Delgass, W.; Ribeiro, F. H. *J. Catal.* **2012**, *289*, 171−178.

(231) Shekhar, M.; Wang, J.; Lee, W. S.; Cem Akatay, M.; Stach, E. A.; Nicholas Delgass, W.; Ribeiro, F. H. *J. Catal.* **2012**, *293*, 94−102.

(232) Cámara, A. L.; Chansai, S.; Hardacre, C.; Martínez-Arias, A. *Int. J. Hydrogen Energy* **2014**, *39*, 4095−4101.

(233) Costa, C. N.; Efstathiou, A. M. *J. Phys. Chem. B* **2004**, *108*, 2620−2630.

(234) Haneda, M.; Nakamura, I.; Fujitani, T.; Hamada, H. *Catal. Surv.Asia* **2005**, *9*, 207−215.

(235) Haneda, M.; Kintaichi, Y.; Hamada, H. *Appl. Catal., B.* **2005**, *55*, 169−175.

(236) Anastasiadou, T.; Loukatzikou, L. A.; Costa, C. N.; Efstathiou, A. M. *J. Phys. Chem. B* **2005**, *109*, 13693−13703.

(237) Lambrou, P. S.; Efstathiou, A. M. *J. Catal.* **2006**, *240*, 182−193.

(238) Savva, P. G.; Efstathiou, A. M. *J. Catal.* **2008**, *257*, 324−333.

(239) Savva, P. G.; Costa, C. N.; Efstathiou, A. M. *Kinet. Catal.* **2008**, *49*, 743−747.

(240) Klukowski, D.; Balle, P.; Geiger, B.; Wagloehner, S.; Kureti, S.; Kimmerle, B.; Baiker, A.; Grunwaldt, J. D. *Appl. Catal., B* **2009**, *93*, 185−193.

(241) Verykios, X. *Appl. Catal., A* **2003**, *255*, 101−111.

(242) Bobin, A. S.; Sadykov, V. A.; Rogov, V. A.; Mezentseva, N. V.; Alikina, G. M.; Sadovskaya, E.; Glazneva, T. S.; Sazonova, N. N.; Smirnova, M. Y.; Veniaminov, S. A.; Mirodatos, C.; Galvita, V.; Marin, G. B. *Top. Catal.* **2013**, *56*, 958−968.

(243) Theologides, C. P.; Olympiou, G. G.; Savva, P. G.; Pantelidou, N. A.; Constantinou, B. K.; Chatziiona, V. K.; Valanidou, L. Y.; Piskopianou, C. T.; Costa, C. N. *Water Sci. Technol.* **2014**, *69*, 680−686.

(244) Balakos, M. W.; Chuang, S. S. C. *J. Catal.* **1995**, *151*, 266−278.

(245) Chuang, S. S. C.; Brundage, M. A.; Balakos, M. W. *Appl. Catal., A* **1997**, *151*, 333−354.

(246) Brundage, M. A.; Balakos, M. W.; Chuang, S. S. C. *J. Catal.* **1998**, *173*, 122−133.

(247) Hammache, S.; Goodwin, J. G. *J. Catal.* **2003**, *218*, 258−266.

(248) Cheung, P.; Bhan, A.; Sunley, G.; Law, D.; Iglesia, E. *J. Catal.* **2007**, *245*, 110−123.

(249) Chansai, S.; Burch, R.; Hardacre, C.; Breen, J. P.; Meunier, F. C. *J. Catal.* **2011**, *281*, 98−105.